Seasonal influences on groundwater arsenic concentrations in the irrigated region of the Cambodian Mekong Delta

S. Tweed, S. Massuel, J.L. Seidel, K. Chhuon, S. Lun, K.E. Eang, J.P. Venot, G. Belaud, M. Babic, M. Leblanc

Seasonal influences on groundwater arsenic concentrations in the irrigated region of the Cambodian Mekong Delta.

Tweed S.[1*], Massuel S.[1], Seidel JL.[2], Chhuon K.[3], Lun S.[3], Eang KE.[3], Venot JP.[1], Belaud G.[1], Babik M.[4], Leblanc M.[4]

[1]UMR G-eau, IRD, SupAgro, Montpellier, France
[2]UMR HSM, University of Montpellier, CNRS, Montpellier, France
[3]ITC, Phnom Penh, Cambodia
[4]UMR EMMAH, Hydrogeology Laboratory, University of Avignon, France

[*]Corresponding author: sarah.tweed@ird.fr

Abstract

Similar to many southern and southeast Asian regions, the mobilisation of arsenic (As) from sediments has driven a widespread contamination problem for groundwater resources in the Cambodian Mekong Delta. For the first time, the seasonal changes in As concentrations and potential links to groundwater pumping for irrigation in shallow aquifers of the Cambodian Mekong Delta are investigated. Using environmental tracers ($\delta^{18}O$, $\delta^{2}H$, ^{3}H, major/trace ions and rare earth elements) the natural and pumping-induced changes in hydrogeological processes are identified. Three conceptual models are proposed: Model 1, where there is limited local recharge or low recharge rates (^{3}H mean residence time > 60 years) and groundwater has a large range in As concentrations (0.2 to 393.8 μg/L). In this semi-confined aquifer, only one of the six groundwater sites has As concentrations that increase (by 10.9 μg/L) potentially due to groundwater pumping and resultant mixing with high-As and low $(Pr/Sm)_{NASC}$ groundwater. However, data on groundwater extraction volumes is required to verify the link with irrigation practices. Model 2, where groundwater is recharged by evaporated surface waters (fractionated $\delta^{18}O$ and $\delta^{2}H$). There are moderate As concentrations (64.1-106.1 μg/L) but no significant seasonal changes even though the recharging waters have relatively greater organic carbon contents during the dry season (reduced Ce/Ce*anomaly). Finally model 3, where groundwater is significantly recharged by wet season rainfall (~50 % from $\delta^{18}O$ data). There is a minor increase in As concentrations with recharge (by 6. μg/L). These combined results highlight an aquifer system in the irrigated region of the Cambodian Mekong Delta where As concentrations are largely impacted by natural rather than irrigation processes. Seasonal-scale recharge processes control As processes where the aquifer is not confined by shallow clay layers, and where the aquifer is semi-confined As concentrations largely reflect longer-term natural processes.

Keywords: groundwater quality, groundwater resources, irrigation, arsenic.

1. Introduction

The impact of irrigation practices on the contamination of groundwater by arsenic (As) is a globally recognised phenomenon. Whilst in many cases As is derived from natural sources, it is well established that groundwater pumping can cause changes to the mixing and biogeochemical processes, and thereby accentuate the As issue in groundwater resources. The extraction of groundwater leading to changes in As concentrations has reportedly occurred in the United States (e.g. Ayotte et al., 2011; Smith et al., 2018), Vietnam (Berg et al., 2008), and Taiwan (Liu et al., 2003).

The main aquifer of the Cambodian Mekong Delta is viewed as a groundwater system that remains under relatively 'natural' conditions in terms of the extent and timing of groundwater pumped for irrigation (e.g. Polya et al., 2005; Polizzotto et al., 2008; Lawson et al., 2013; 2016). Therefore, the effects of groundwater pumping for irrigation on the As crisis in the Cambodian Mekong Delta has not received the same attention compared to other southern and southeast Asia regions. For example, in Bangladesh where the consequences of As contamination on public health are the most severe worldwide (e.g. Raessler, 2018) there are several models proposed for the As release in groundwater in irrigation regions. Many studies have hypothesised that irrigation withdrawals of groundwater are the cause of elevated As concentrations in aquifers (e.g. Harvey et al., 2002). It is suggested that pumping promoted As mobilisation in groundwater through the increase in hydraulic gradients that allow the transfer of young surficial organic matter to reach greater depths in the aquifer compared with 'natural' conditions (Neumann et al., 2010). Radloff et al. (2017) also found that the sorption and desorption processes within the aquifer during pumping can rapidly affect As mobilisation in groundwater, and for the aquifer sands in the Bengal Basin this was not highly sensitive to changes in the As redox state. In comparison, Mailloux et al. (2013) analysed a site in Bangladesh where reductions in hydraulic heads due to pumping and resultant increases in recharge

66 did not significantly influence groundwater redox, and it was concluded that the As mobilisation was
67 due to natural long-term processes pre-dating human perturbations.
68
69 Despite lower groundwater extraction rates in the Cambodian Mekong Delta compared with other
70 As-affected regions of southeast Asia (Lawson et al., 2013), many farmers and rural inhabitants are
71 dependent on groundwater resources, particularly during the dry season. Groundwater from shallow
72 aquifers in the upper delta region represents a strategic resource to people who cannot rely on
73 surface water, for both supplementary domestic use or for irrigation. Land irrigated by groundwater
74 in this region has reportedly increased by ~10% per year over the period 2003-2015 (Erban and
75 Gorelick, 2016). In the Vietnam Mekong Delta, a study found that the pumping of deep confined
76 aquifer systems causes inter-bedded clays to compact and release either As into solution, or release
77 dissolved organic carbon and competing ions that help to mobilise As (Erban et al., 2013). However,
78 this was an investigation of a deep aquifer system and to the best of our knowledge, the irrigation
79 pumping impacts on As in shallow aquifers of the Cambodian Mekong Delta have not yet been
80 documented.
81
82 In the Cambodian Mekong Delta, many previous studies have established that the major As
83 mobilisation processes in the shallow aquifers include the microbial decomposition of organic
84 matter and the reductive dissolution of arsenic-bearing iron minerals (Fe(III) oxyhydroxides) under
85 anaerobic conditions (Pederick et al., 2007; Rowland et al., 2007; Polizzotto et al., 2008; Quicksall et
86 al., 2008; van Dongen et al., 2008; Lawson et al., 2013; 2016; Richards et al., 2017a; 2019). However,
87 there are many different models that describe the environmental context of these processes. For
88 example, since labile organic carbon is essential for the mobilisation of As in aquifers, there have
89 been many studies devoted to analysing the sources and transfers of this carbon. In the Cambodian
90 Mekong Delta, studies have highlighted the multiple sources of organic carbon from both in-aquifer
91 sources (van Dongen et al., 2008) and surficial sources (Lawson et al., 2013; 2016; Richards et al.,

2019), which is used in the reductive dissolution of arsenic-bearing iron minerals (Fe(III) oxyhydroxides) that mobilises As in groundwater. The release of As has also found to be slower where the source of organic matter is from sediments that are older and deeper, compared with recently recharged near-surface organic carbon (Polizzotto et al., 2008). Therefore, the hydrodynamics of an aquifer, and modifications thereof, can significantly influence the rates of As mobilisation in groundwater.

In this study, we build on the extensive As investigations already undertaken in the Cambodian Mekong Delta (see Richards et al., 2019), by providing the first conceptual model of the seasonal-changes in As concentrations in the shallow aquifer of the irrigated region. Groundwater from typical rural sites was analysed where the resource is used for both irrigation and domestic use purposes. In this study we investigate shallow groundwater along a 40 km length of the Bassac River, the river that stems from the Mekong mainstream in Phnom Penh at the apex of the delta. There are currently no groundwater monitoring bores or on-going measurements of hydraulic heads in this region, therefore we use environmental tracers (stable isotopes, major ions, trace elements, rare earth elements and tritium) to help identify key hydro(geo)logical processes. The study objectives are to analyse (i) the origins of groundwater pumped for water supplies; (ii) the seasonal-scale changes in groundwater chemistry; and (iii) whether or how the As concentrations seasonally change during the dry season when groundwater is used for irrigation.

2. Study Area

The study area is located in the Kandal province of the Cambodian Mekong Delta, situated between Phnom Penh and the border with Vietnam (Fig. 1). The tropical monsoon climate in this delta is

117 characterised by high wet season rainfall volumes derived from southwestly weather systems, and a
118 dry season that is dominated by northeasterly weather systems (Briese, 1996).
119
120 **2.1 Hydro(geo)logy and aquifer geology**
121 South of Phnom Penh the Mekong River diverges to form the Bassac River that runs in parallel with
122 the Mekong River until they both discharge to the South China Sea in Vietnam. In the Cambodian
123 Mekong Delta, the rivers have high seasonal variations in water levels due to the large seasonal
124 differences in rainfall levels between the wet and dry seasons. For example, the Bassac River has
125 fluctuations in water levels of up to 6.6 m (between 1990-2018; Fig. 2a). Due to the flat topography
126 of the delta there are large areas that are annually inundated during the wet season rise of the river
127 water levels. Additional influences to the river water levels include tidal changes, groundwater
128 baseflow during the dry season (e.g. Rasmussen and Bradford, 1977; Polizzotto et al., 2008), and
129 river recharge to the aquifer during the wet season (e.g. Richards et al., 2018). In the study area, it
130 remains unclear whether the Bassac River interacts with shallow groundwater along its length, or
131 whether this is a spatially variable phenomenon limited by the thickness and continuity of the
132 underlying confining clay-rich sediments (as is the case in the Vietnamese section of the Mekong
133 Delta). The Bassac River has also been deepened in recent years due to river-bed mining (e.g.
134 Bravard et al., 2013), which has caused pools of up to 15 m deeper than the natural level (Brunier et
135 al., 2014; Anthony et al., 2015).
136
137 The sediments underlying the Bassac River are comprised of Quaternary alluvial sediments
138 deposited under river and marine environments. These sediments form stratified deltaic layers of
139 sand, gravel, clay and silt, and are regionally divided into two groups: the old (Pleistocene) and
140 young (Holocene) alluvium. The younger Holocene alluvium outcrops across the low elevation region
141 of the delta (<10 m ASL). In the study area this younger alluvium is the clay-rich confining layer that
142 can reach a thickness of up to ~18 m (Rasmussen and Bradford, 1977); the thickness increases

towards the Vietnamese coast reaching a maximum of > 100 m (Anderson, 1978). Underlying the younger alluvium is the older Pleistocene alluvium, which in comparison contains less clay, coarser material (sand, gravel, pebbles), and is therefore the major shallow aquifer. In the Cambodian section of the delta the aquifer can be up to 100-120 m deep, whereas in the lower delta in Vietnam the thickness reaches up to 450 m (Briese, 1996). Bedrock underlies and borders these alluvial sediments, and in cases such as the basalt intrusions the bedrock is also interbedded with the old alluvium. The bedrock is comprised of igneous, metamorphic and consolidated sedimentary rocks that range in age from Precambrian to Plio-Pleistocene (Anderson, 1978). Underneath the Bassac River the basement bedrocks are over 160 m from the surface (JICA, 2002).

Regionally groundwater flow in the delta is towards the south (Briese, 1996). Although groundwater is an important water resource in the delta there are very few bores monitored for hydraulic head data. Previous studies have identified that groundwater levels are relatively low in June and July, and increase by ~5m in October and November (JICA, 2002). In the northern region of the Kandal Province previous studies have highlighted that groundwater close to the river is heavily influenced by river water level fluctuations, with the river's influence on groundwater levels decreasing with distance and depth (Polizzotto et al., 2008; Richards et al., 2017a). However, the spatio-temporal variations in groundwater elevations throughout the Cambodian Mekong Delta, particularly due to groundwater pumping, are very poorly documented. The clay-rich sediments of the younger alluvium forms a confining layer at the surface resulting in the underlying old alluvial aquifer acting as a semi-confined system.

As in many developing countries, in both semi-arid and wet tropical environments, groundwater resources in the Cambodian Mekong Delta are essential to rural communities (e.g. about 3,000 private wells have been identified in the study area by the Water Sanitation Program (WSP, 2019)). Although groundwater resources are of poorer quality compared with river water in terms of

electrical conductivity and arsenic (see below results from this study), it is an unmonitored water resource, and there is a cost associated with installing groundwater bores, many rural inhabitants rely on accessing groundwater for both agricultural and domestic (including drinking) uses.

2.2 Irrigation

This region of the Mekong Delta is dedicated to farming that is heavily dictated by the wet and dry seasons and the topography. Land along the river banks is slightly elevated then gently slopes down in a perpendicular direction towards low-lying wetlands located further away from the main river streams. Close to river banks, farmers can cultivate yearlong; orchards and vegetables dominate the landscape and are irrigated especially during the dry season (Feb-May). Further away from the river, farmers cultivate up to two crops of short term rice (e.g. 90-95 days crop). The first season starts when the flood recedes (in November/December; this is locally called recession rice) and is mainly rainfed though supplementary irrigation is common. For the second season, the cropping calendar differs based on topography and water availability. Some farmers (low lying, more water available, and higher vulnerability to floods) cultivate and irrigate rice during the dry season (Feb-May; this is locally called dry-season rice), while others (slightly more elevated, less water available but less vulnerable to floods) start cultivating rice in May with the first rains and harvest before the floods come towards the end of July (supplementary irrigation is still needed; this is locally called early wet season rice; Pillot, 2007).

In support of the agricultural activities in the study area there is a dense network of earthen artificial channels locally call preks, acting as drainage and irrigation canals (SOFRECO, 2019). The beds of these channels were usually dug several meters below the land surface, perpendicularly to the Bassac, on a length of about 4 km, and are spaced 0.5 to 1 km (Fig. 1b). During high river water flows the channels divert the water and sediments inland, and can either link the Bassac River with other

natural river streams in the delta or the water and sediments culminate in the low lying wetlands. The same channels drain water back to the river during low river flow periods. The canals are used for transportation, fishing and are also a major source of irrigation water (with farmers installing small diesel pumps to draw water from the canals to their fields).

There has been recent rehabilitation (including deepening) of some irrigation channels in this region of the delta to improve the water control and availability. Some channels were equipped with gates, managed by water user associations to regulate flow from or to the river. In some cases, floating pumping stations were installed on the Bassac and water is pumped in the channel during dry season. Despite these changes, many of the irrigation channels (60% in 2018; SCP, 2018) cannot provide river water inflows all year round, especially during the driest months. Many farmers are obliged to install their own groundwater bores in order to irrigate during the dry season and for domestic purposes. Groundwater is used for the irrigation of vegetables, fruit tree farms and rice fields, and is mostly pumped at the end of the dry season for irrigation (~ May/June, depending on the year).

2.3 Arsenic

In the Cambodian Mekong Delta, groundwater has been used to irrigate rice fields since ~ 1984 and in areas where groundwater is the primary source of irrigation water the concentration of As in the soils is elevated, albeit with lower health risks compared with the higher toxicity of arsenic present in rice cultivated in Bangladesh (Murphy et al., 2017). For example, in the Kandal province Murphy et al. (2018) reported As concentrations in soils close to wells that were approximately double the concentrations of soils further from the well. Although groundwater is an essential dry season water resource, it is well established (e.g. Phan et al., 2013) that As in groundwater is a health threat to the rural population in the Cambodian Mekong Delta. Accordingly, As has received a lot of national attention (e.g. database of 59000 records of As in groundwater in Cambodia; WSP, 2019). However,

in part because of the lack of in-situ groundwater monitoring data, this As database has not been analysed in combination with the modified hydro(geo)logical processes due to irrigation practices. In addition, as discussed previously, the natural processes influencing As concentrations are already numerous and complex; including the non-uniform distribution of the eroded Himalayan sediments, competing electron acceptors, and the reactivity, age and transfers of organic carbon (Papacostas et al., 2008; Quicksall et al., 2008; Lawson et al., 2016; Richards et al., 2017b). An additional potential source of As in the study area is the use of fertilisers. However, a recent study in Kandal by Murphy et al. (2018) calculated that As loads in groundwater used for irrigation were over 3000 times the As loads present in the inorganic fertilisers being used.

3. Methods

In this study, a new As dataset is analysed in conjunction with hydrochemical tracers to inform us on the hydro(geo)logical processes in areas where groundwater is used for irrigation. Here we analyse river bathymetry data in conjunction with hydrochemical parameters to study the potential interactions between the river and shallow groundwater. The hydrochemical tracers are also used to identify hydrogeological processes affecting As concentrations. Field visits were conducted during June and September in 2017 and 2018 (Fig. 2b). Samples in June represent the end of the dry season/start of the wet season, and it is during June that we expect to see the full impacts of the dry season pumping on shallow groundwater samples. In comparison, samples collected in September represent the peak of the wet season.

3.1 River bathymetry and flow

River bathymetry data was used to map sections of the river bathymetry and flow velocity from one bank to the other (back and forth). The ADCP was coupled with a differential GPS in order to map

247 the exact profile track perpendicular to the riverbed. Then, the entire river flow through the section
248 was inferred. During the dry season, an acoustic Doppler current profiler (ADCP, RDI™ 600 kHz) was
249 used to map sections of the river bathymetry and measure the river flow at the northern (R10) and
250 the southern (R1) sites. In addition, a hand held pressure sensor was used to record the river depth
251 (surface water level elevation minus water column) at each of the sampling sites along the length of
252 the Bassac River. The same protocol was repeated during the wet season, but a pressure sensor was
253 also used to map sections of the river bathymetry at three locations. The mean river bed minimum
254 elevation was about 5m below sea level, but deeper sections were observed in meanders. Such low
255 elevations of river depths are not uncommon in the study area, for example previous work by Lu et
256 al. (2014) found sections in the Mekong River up to 15m below the sea level. Water level variations
257 (Fig. 2) are monitored by Mekong River Commission on a daily basis at Koh Khel (11°16'8"N, 105°
258 1'40.5"E), and on hourly basis at Chau Doc (10°42'26"N, 105° 7'38"E) at the south of the study area.
259
260 **3.2 Hydrochemistry of surface water and groundwater**
261 The lack of physical hydrogeological time-series data in the study area necessitated the use of
262 environmental tracers (major ions, stable and radiogenic isotopes, and rare earth elements) to help
263 analyse the origins and transfers of groundwater. In 2017, 10 surface water sites (including water in
264 the prek channels used for irrigation or drainage water, water from low lying wetlands (floodwater),
265 and river water) were sampled during the dry and wet seasons, and in 2018 10 groundwater and 10
266 river sites along ~40 km of the Bassac River were sampled during the dry and wet seasons (Table 1).
267
268 The locations of the groundwater and surface water samples are presented in figure 1b and c. The
269 groundwater sites were selected to represent locations close to the river's edge; all groundwater
270 samples are located at distances of 0.3-1 km from the Bassac River's edge. In addition, the sites were
271 selected based on their location within irrigated areas; privately owned bores were sampled that are
272 actively used for domestic (including drinking water supplies) and/or irrigation purposes. The

273 groundwater samples were collected using the pumps already installed in the privately owned bores
274 that pumped groundwater from near the base of the bore. The depths for the groundwater bores
275 sampled range from 18-62 m and are presented in Table 1. The bores are screened along the length
276 of the casing. Therefore sampling depths will vary depending on pumping rates and changes in
277 hydraulic conductivity values of the aquifer with depth. Groundwater bores were pumped until the
278 EC stabilised, after which the field parameters were measured and samples were collected for
279 laboratory analysis. All river samples were collected at ~50 cm depth from the middle of the river
280 using a boat. For both river and groundwater samples the electrical conductivity (EC), pH and
281 temperature were measured in the field using the field-calibrated meter WTW 3320. Water samples
282 were collected in the field for major, minor and trace elements, stable isotopes and tritium.
283
284 The major and minor ions, and stable isotopes were analysed at the Hydrochemistry Laboratory,
285 University of Avignon, France. Samples for ion analyses were filtered in the field (0.45 μm cellulose
286 nitrate filter) and an aliquot was acidified to pH < 2 (ultrapure 16N HNO_3). Anions and cations were
287 analysed using ion chromatography (Dionex; ICS1100) and ion analysis uncertainty is in the order of
288 3 %. For ion analysis, the quality control methodology is performed by cross-calculations of
289 conductivity, ion balances and saturation indices for each dataset. In addition, inter-laboratory
290 analyses are regularly undertaken. For the concentrations of N species we used groundwater
291 sampled in the Vietnam Mekong Delta to compare values (i) when analysed locally within a couple of
292 days by standard colorimetric methods and (ii) when the filtered samples were analysed a few
293 weeks later in France at the University of Avignon (ion chromatography), which is the same
294 laboratory used in this study. The results varied slightly (differences in NH_4 ≤2.71 mg/L) and the
295 differences were linear (e.g. for NH_4 R^2= 0.953); therefore we consider that the relative changes of
296 NH_4 between different groundwater samples in this study will still be valid. However, we use a
297 higher detection limit of 2 mg/L for NH_4 than the analytical detection limit associated with the ion
298 chromatography analysis (0.01 mg/L). Results of selected cations and anions for groundwater and

surface water are presented in Table 1. Charge balance errors for these waters are ≤ 5 %. Stable isotope values (δ^2H and δ^{18}O) were analysed using the LGR (Los Gatos Research) laser spectrometer; the uncertainty is δ^{18}O = ±0.1‰ and δ^2H = ±1‰ (Table 1).

Samples were also analysed for Tritium (^{3}H) contents (Table 1) by low level liquid scintillation counting after electrolytic enrichment using a scintillation counter (Tri-Carb 3180 TR/SL) at the Hydrochemistry Laboratory, University of Avignon, France. Calibration of the device was undertaken before analysis of these water samples, during analysis there are control samples (of "dead water") in conjunction with regular inter-comparison with IAEA analysis and monitoring the enrichment factor of each electrode. The results are returned to 2-sigma and the uncertainty associated with ^{3}H results ranges from 0.3to 0.6 TU (Table 1). For four groundwater samples there is ^{3}H present but the values are low (0.8-1.2 TU), and for most groundwater samples the ^{3}H activities were below the detection limit. For these samples below the detection limit, the ^{3}H value noted in Table 1 is ≤ the 2-sigma error associated with the sample analysis (e.g. ≤ 0.7 TU for G1 in June). Consequently, although during the analysis the average counts per minute (cpm) of the June G1 sample was less than the cpm of the "dead" ^{3}H water and the detection limit at 2σ, and the average cpm of the September G1 sample was greater, due to the 2σ error value we cannot say that the ^{3}H value of ≤ 0.7 TU in June is significantly different to 0.8 ± 0.3 TU in September.

The trace element and rare earth element samples were filtered (0.2 μm) and acidified to pH < 2 (ultrapure 16N HNO_3) in the field. The samples were then analysed at the AETE-ISO platform OSU-OREME at the University of Montpellier, France, with an ICAP Q THERMO SCIENTIFIC. Trace element and rare earth element results are presented in Table 2. For the June groundwater trace element data presented in Table 2 a repeat analysis was undertaken, and t-test p-values were > 0.05 indicating that the two analyses were not significantly different. For trace element analysis, all chemicals used were of analytical grade (Merck Darmstadt, Germany). Ultrapure water was used throughout the analysis. For calibration, multi-elemental standard solutions of metals were

prepared by dilution of a 1000 ppm certified standard solution (SCP Science, Canada) of corresponding trace elements. Instrumental drift was monitored and corrected by addition of a multi-elemental (Be, Sc, Ge, Rh, Ir) internal standard to each sample. Reagent and procedural blanks were measured in parallel to sample treatment using identical procedures. Participation in laboratory inter-comparison exercise was achieved for CRM SLRS-5 (Yeghicheyan et al., 2013) and for SLRS-6 (Yeghicheyan et al., 2019) to complete the quality control methodology. The accuracy of the data was tested by replicate analyses of the certified river water reference standard SLRS-6 for trace elements (National Research Council, Canada). SLRS-6 was analysed every 10 samples to test the analysis accuracy and precision. The SLRS-6 results are within the range of certified uncertainties and deviations from the certified values were generally lower than 10% except for Pr (12%) and Tm (13%). Repeated analysis of the CRM SLRS-6 several months apart makes it possible to assess the reproducibility and the long-term precision of the analyses for each element (Table 3). The total errors ($\sqrt{(\text{sample error}^2 + \text{analytical error}^2)}$) for As are presented in Table 2 and are used in the comparison of the seasonal changes in As concentrations at each site.

3.3 Geochemical modelling

Two-component mixing models were used to determine (i) the relative recharge to the aquifer from wet season rainfall at site G1, and (ii) the relative recharge of evaporated water compared with rainwater for each of the groundwater sites. The first model used to calculate wet season rainfall recharge at site G1 is based on those described in Clark and Fritz (1997) and uses equation (1):

$$F_r = (C_{mix} - C_{gw}) / (C_r - C_{gw}) \quad (1)$$

Where the fraction of rainfall contribution to the groundwater aquifer (F_r) at site G1 is calculated using the concentrations of the tracer for groundwater from the aquifer before recharge (C_{gw}), the

groundwater after recharge (C_{mix}), and for the rain water (C_r). Calculations were undertaken using the stable isotope $\delta^{18}O$ values.

The second mixing model, used to calculate the fraction of evaporated pond waters recharging groundwater (F_{evap}) with equation (2), was also used by Richards et al. (2018) in the Kandal province ~20 km north of our study area.

$$F_{evap} = (C_{gw} - C_r) / (C_{evap} - C_r) \quad (2)$$

The calculations use both $\delta^{18}O$ and $\delta^{2}H$ data. Equation 2 uses the isotope values of groundwater (C_{gw}), end-member isotope values of rain (C_r) and end-member isotope values of evaporated water (C_{evap}). The end-member isotope values for rainfall were those values used by Richards et al. (2018) from 2014 rainfall data collected in Kandal ($\delta^{18}O$ = -10.6, $\delta^{2}H$ = -69.5 ‰). The end-member isotope values for evaporated water were collected in this study from a drainage pond ($\delta^{18}O$ = -0.81, $\delta^{2}H$ =18.44 ‰). Results of this modelling are presented in Table 1 for all groundwater sites. Where the modelled % of groundwater sourced from evaporated water are > 65%, these indicate areas where the waters are more evaporated than mean rainfall values (Richards et al., 2018).

4. Results

4.1 River flow and depth profiles

In the dry season, the river discharge was measured at 660 m^3/s along the upstream profile and 470 m^3/s downstream. In the wet season, the upstream flow was 2700 m^3/s and 1650 m^3/s downstream. This means that the discharge was reduced by 30% and 40% along the 40-km length of the Bassac River in the dry and wet season respectively. The discrepancy of the flow can be attributed to water being discharged through the channels towards the floodplain. It can also be the

result of a net contribution from the river to the underlying aquifer in wet season (i.e. when the hydraulic gradient is towards the aquifer). . The measurements showed that the bathymetry of the streambed was heterogeneous with depths up to 13 m below ground surface at locations R1, R10 and between R4 and R5, creating possible connections between the river and the semi-confined aquifer.

4.2 Stable isotope values of groundwater and river water

There does not yet exist an extensive database for stable isotopes of local rainfall in the lower Mekong Delta (Cambodia and Vietnam). The LMWLs used in this study include data from 2014 rainfall in the Kandal province (Richards et al., 2018) that has a lower slope (6.4) compared with the LMWL from long time-series rainwater data (1968-2015) collected in Bangkok (slope 7.3) located ~500 km NW of the study area (GNIP station 4845500, elevation 2 mASL, 460 samples). Stable isotope data of rainfall at Bangkok is considered representative of both inter-annual and seasonal variations of rainfall in the lower Mekong Delta (Le Duy et al., 2017). The Bangkok LMWL has a slope that is slightly lower (7.35) compared with the GMWL slope (8) from Craig (1961). In wet and dry tropical zones the seasonal changes in atmospheric moisture transported over continental land mass, temperatures and precipitation volumes result in wet and dry season differences in rainfall stable isotope values (Aggarwal et al., 2004). The average stable isotope values for rainfall at Bangkok during the peak wet season (September and October; 93 samples) are depleted compared with peak dry season values (February and March; 63 samples) that show differences of 6.1 and 45 ‰ for $\delta^{18}O$ and $\delta^{2}H$ respectively (Fig. 3). The Mekong River water sampled in the study region is also influenced by rainfall from the northern area of the Mekong River Basin, where seasonal isotopic differences are further pronounced and show more depleted values. For example, at Kunming (GNIP station 5677800), located 300 km east of the Mekong River Basin in China at an elevation of 1892

401 mASL, the wet season averages for $\delta^{18}O$ and $\delta^{2}H$ are depleted by 9.4 and 61 ‰ respectively
402 compared with the dry season values (data from 1999-2003; Fig. 3).
403
404 Results from this study show that with the exception of groundwater from sites G7 and G8, all
405 samples lie on the meteoric water lines and the dry season groundwater stable isotope values ($\delta^{18}O$
406 = -8.6 to -7.6; $\delta^{2}H$ = -60 to -53 ‰) are only slightly lower compared with dry season river values ($\delta^{18}O$
407 = -7.9 to -7.8; $\delta^{2}H$ = -55 to -54 ‰). During the wet season the groundwater values remain the same
408 as the dry season (maximum change of $\delta^{18}O$ and $\delta^{2}H$ by 0.1 and 1 ‰ respectively), with the
409 exception of site G1 where there was a decrease of $\delta^{18}O$ and $\delta^{2}H$ by 1.2 and 4 ‰ respectively. This
410 indicates either that groundwater and dry season river waters are recharged by similar rainfall
411 sources, or that there are significant inflows of groundwater from this aquifer to the river during the
412 dry season. The results also indicate that groundwater was recharged under similar conditions to the
413 modern day climate. In contrast to the constant groundwater isotope values, the river values
414 increase during the wet season by 0.4-0.6 and 3-5 ‰ for $\delta^{18}O$ and $\delta^{2}H$ respectively. Since the
415 southern region of the Mekong River Basin (e.g. in Cambodia) generally has rainfall with higher
416 isotope values compared with northern region of the Mekong River Basin (e.g. in China), this wet
417 season increase in the river values may correspond with greater contributions from local rainfall.
418
419 Most groundwater shows no evidence of evaporation effects, with the exception of groundwater at
420 sites G7 and G8. Here there is fractionation from the meteoric water lines (Fig. 3) that may result
421 from either evaporation of the groundwater or mixing with evaporated water (Clark and Fritz, 1997).
422 The slope of the regression line for groundwater at these bores is 5.94, which is relatively high and
423 typical of evaporation in a highly humid (> 75%) environment (Clark and Fritz, 1997). The relative
424 extent of evaporation of groundwater calculated for G7 and G8 are higher (65-80 %) compared with
425 all other groundwater sites for both the wet and the dry seasons (≤ 32 %; Table 1). Much of the
426 delta area in Cambodia is naturally inundated during the wet season and artificially inundated during

the dry season from irrigation water. Stable isotope values of all inundation waters are presented in figure 3, and those collected from drainage and irrigation prek waters during the dry season show evaporated signatures with a similar slope (5.29) and values to the groundwater samples from bores G7 and G8 (Fig. 3). In addition, the area is protected by a dyke, but in 2018 the water went through and could not drain back. Therefore, groundwater at G7 and G8 is potentially recharged by evaporated surface waters causing the shift in groundwater isotope values to the right of the MWL. Recharge of evaporated surface waters is consistent with the tritium data (below) which indicates there is recent recharge at these sites, and the major ion chemistry (below) that does not indicate on-going evaporation controls on groundwater chemistry.

4.3 Major ion composition of groundwater

Most groundwater sampled has EC values between 86 to 1207 μS/cm, which increases with borehole depth (Fig. 4a). At site G3 the borehole is deeper (62 m depth from surface) compared with other samples, and has EC values ranging from 4110 to 4220 μS/cm. Despite the increase in rainfall, inundation waters and high river water levels during the wet season, the wet season groundwater EC values do not systematically decrease; only 3 groundwater sites show wet season decreases in EC (by 44 - 506 μS/cm; G1, G6, G9). On the contrary, 3 groundwater sites show increases in EC (by 50 - 110 μS/cm; G2, G3, G5) and 3 sites show no significant seasonal change in EC (< 10 μS/cm; G4, G7, G10). These results indicate the processes controlling groundwater EC are highly spatially and temporally variable.

When compared with stable isotope values, there are 3 distinct end-members with varying EC values (Fig. 4b). At site G1 groundwater is recharged by recent rainfall or inundation waters resulting in isotope and EC values that decrease during the wet season (EC from 592 to 86 μS/cm). The second end-member is from the deeper groundwater borehole at site G3; where isotope and EC values

453 show little seasonal variation (4110 to 4220 μS/cm). Thirdly, the sites G7 and G8 are where
454 groundwater is recharged by evaporated surface water although EC remains low (248 – 293 μS/cm).
455 From these end-members, there are 2 major mechanisms resulting in increases in groundwater EC;
456 (i) due to mixing with evaporated surface waters, and (ii) due to mixing with groundwater that has
457 high EC from water-rock interactions or evapotranspiration. In addition, river waters show increased
458 EC values and decreased isotope values during the dry season highlighting the increase in inflows
459 from groundwater (Fig. 4b).
460
461 Most of these circumneutral pH groundwater samples show some evidence of water-rock
462 interactions with silica concentrations that are up to 10 % of the TDS, and range from 2.9 – 29.4
463 (average = 14.4) mg/L SiO_2 (Table 1). The water-rock interactions results in groundwater
464 characterised by HCO_3-Ca-Mg for most groundwater samples with EC values < 700 μS/cm, except for
465 bore G10 which has notably higher concentrations of SO_4 (457 to 473 mg/L) compared with other
466 ions. Where groundwater has higher EC values (4110 - 4220 μS/cm; G3) there are relative increases
467 in Na and Cl concentrations compared to other major ions.
468
469 Nitrogen in the groundwaters in the study area is mostly < 2mg/L, but there are three groundwater
470 sites that have relatively high ammonium concentrations (NH_4 = 8-23 mg/L; G4, G5, G6). Prek waters
471 and floodwaters also have relatively high NH_4 concentrations (6-38 mg/L) compared with river NH_4
472 concentrations that mostly remain < 2 mg/L (Table 1). NH_4 is present in reducing waters and can
473 originate from either natural sources such as the anaerobic decomposition of organic material, or
474 anthropogenic sources including fertilisers and animal or human sewerage. Anthropogenically
475 sourced NH_4 in groundwater can therefore highlight infiltration of water from the surface or shallow
476 sub-surface. Cl/Br molar ratios higher than seawater values (~ 650 to 660; Davis et al., 1998) relative
477 to a large range in Cl concentrations (Cl/Br: 620-1970, Cl: 35-396 mg/L) can indicate contamination
478 of water from human sewerage and septic tank effluent (e.g. Katz et al., 2011). Many groundwater

479 samples in this study have Br concentrations below detection limits, and those values measured
480 show that Cl/Br molar ratios that remain relatively low (340-746; Table 1), including samples G5 and
481 G6 (Cl/Br ratios 464 and 592 respectively) that have relatively high NH_4. This indicates little
482 contamination from anthropogenic wastewater in the aquifer. In comparison, the irrigation and
483 drainage prek waters have elevated Cl/Br molar ratios ranging from 628-947 (Table 1), which may
484 indicate some influence of NH_4 from fertilisers or animal/human sewerage. Therefore, a high
485 component of NH_4 in the groundwater is likely sourced from the anaerobic respiration of organic
486 material, which is discussed further below in relation to arsenic concentrations.
487
488
489 **4.4 Tritium content**
490 The river ^3H results show seasonal differences with values higher in the dry season (mean = 2.5 TU;
491 range = 2.3-2.9 $\pm$ 0.3-0.6 TU) compared with the wet season (mean = 1.9 TU; range = 1.8-2.5 TU $\pm$
492 0.3-0.5). Higher values can indicate increased contributions from rain in the northern region of the
493 Mekong River Basin during the dry season (Nguyen et al., 2007), which is consistent with the stable
494 isotope value results. Rainfall ^3H data shows that although the atmospheric contents were 10 times
495 lower than those experienced in European rainfall during the nuclear bomb pulse effect, SE Asia also
496 experience elevated atmospheric ^3H contents during the 1960s that have since declined to values
497 consistent with pre-bomb pulse conditions.
498
499 The ^3H contents of groundwater sampled in this study show that most samples were predominantly
500 recharged prior to the 1960s ($^3H \leq 0.3$ to ≤ 0.8 TU; Table 1). These results indicate that there was not
501 enough recent recharge from rainfall, inundation waters, irrigation waters or river water observed
502 over the seasonal scale for the apparent tritium content of the bulk sample to be above the
503 detection limit. This therefore highlights a relatively shallow aquifer system (depth ~ 30-40 m) that is
504 semi-confined. In terms of river-groundwater interactions, because there is no detectable ^3H in most

505 groundwater samples this implies that either (i) the sites are outside of the zone of influence of river
506 inflows to the aquifer, which is kept small by the seasonal reversals in hydraulic gradients, or (ii) the
507 river does not sufficiently cut through the aquitard to interact with the semi-confined aquifer.
508
509 At sites G1, G7, and G8 there is some ^{3}H detected, however the activities are considered too low to
510 significantly different from the other groundwater samples. At site G1, the low ^{3}H in the wet season
511 (0.8 $\pm$ 0.3 TU) is not significantly greater than values in the dry season (≤ 0.7 TU), even though
512 changes in major ion chemistry highlighted a wet season dilution due to recharge by rainfall or
513 inundation waters. At the site G7 there is some ^{3}H present during both the dry season (1.2 $\pm$ 0.3 TU)
514 and the wet season (0.8 $\pm$ 0.4 TU), however this is also not significantly different to groundwater
515 samples where the 3H value is below detection, and similar at site G8 where there is a low activity of
516 ^{3}H during the dry season (1.2 $\pm$ 0.4 TU; wet season analysis was not possible due to the site being
517 inundated). The stable isotope and major ion data suggest that the water recharging the aquifer at
518 sites G7 and G8 is evaporated. This in addition to the lack of significant seasonal change in ^{3}H at G7
519 indicates that the recharge rates do not significantly differ between dry and wet seasons.
520
521
522 **4.5 Arsenic in groundwater**
523 All Bassac River arsenic (As) concentrations are relatively low, with wet season values (0.7-1.3 μg/L)
524 slightly lower than dry season values (1.3-1.5 μg/L). In comparison, groundwater shows a larger
525 range in concentrations, with five groundwater sites that have As values below the 10 μg/L limit that
526 WHO (2017) provides as a provisional guide for drinking water (0.2 to 8.6 μg/L; Table 2), and one
527 groundwater site that has As values below the 50 μg/L limit that the Cambodian government uses (≤
528 14.6 μg/L). In comparison, the 4 other groundwater sites have high As concentrations above both
529 the WHO and Cambodian government limit (64.1 – 393.8 μg/L; Table 2). Where the mean residence
530 time of groundwater is > 60 years the concentrations of As are higher (sites G4 and G5: As = 218.5-

393.8 μg/L) compared with sites where the groundwater has younger residence times (< 60 years at sites G7 and G8; As = 64.1-106.1 μg/L).

When taking into account the total errors of As (Table 2), there are only two sites that show significant changes in As concentrations between the dry and wet seasons (Fig. 5). Site G6 shows an increase in As by 10.9 μg/L during the dry season. Whereas site G1 shows an increase in As by 6.8 μg/L during the wet season. All other sites show no significant seasonal change in As concentrations (Fig. 5).

In comparison with other trace elements, the seasonal increases in As concentrations predominantly corresponds with a seasonal decrease in manganese (Mn, R^2 = 0.5) compared with a positive correlation with iron (Fe, R^2 = 0.5; Fig. 6). For most groundwater, with both high and low As concentrations, the HCO_3 concentrations remain relatively high and the SO_4 concentrations are generally low (≤ 3 mg/L; Table 1). These results are indicative that reductive-dissolution of Fe oxides/hydroxides is a driving process of high As concentrations in groundwater.

4.6 Rare earth elements

The results of the rare earth element (REE) concentrations are presented relative to the North America Shale Composite (NASC) in figure 7. For the Bassac River, the high REE concentrations during both the wet and dry seasons (Fig. 7a) indicate some interactions with the sediment load. There are small decreases in Cerium (Ce, where Ce/Ce* = 0.6-0.8; Table 2), which is common because of the propensity for this REE to be preferentially removed from solution in oxygenated river water (e.g. Leybourne and Johannesson, 2008). However, the sediment interactions do not significantly change overall REE patterns, which remain flat relative to NASC. The minor seasonal

556 variations and relatively high REE concentrations compared with groundwater samples suggest that
557 groundwater inflows to the river are not detected by the REE concentrations.
558
559 The only groundwater site that resembles river REEs is at G1 during the wet season (Fig. 7a). Other
560 hydrochemical parameters, as presented above, show that this site is significantly recharged by wet
561 season rainfall and not by the river. Therefore, the similar REEs to river values at G1 are likely a
562 reflection that there are limited water-rock interactions occurring between the recharging water and
563 the lithology in the wet season. During the dry season, site G1 has a similar REE pattern to many
564 other groundwater sites where there are small increases in heavy REEs (HREEs) relative to light REEs
565 (LREEs; Fig. 7a). For example, groundwater has greater $(Yb/Nd)_{NASC}$ ratios (0.7-9.8) compared with
566 the stable river patterns (0.9-1.5; Table 2). Increases in HREEs can result from mineral dissolution
567 reactions, the preferential sorption of light LREEs (e.g. Biddau et al., 2002), and/or due to the
568 complexation of more stable HREEs in groundwater of circumneutral pH (e.g. Johannesson et al.,
569 2000). Most REEs patterns for groundwater also exhibit a downward concave pattern for the medium
570 REEs (MREEs; Fig. 7), which can be indicative of a high organic matter content of the REE sources
571 (e.g. Pouret et al., 2007; Davranche et al., 2015).
572
573 In addition to the seasonal variations observed at site G1, the groundwater sites G7, G9, G4 and G6
574 (Figs. 7b-d) also show changes in REEs between wet and dry seasons. Sites G7 and G9 both show a
575 wet season decline in the Ce/Ce* ratios by 0.5, which is accompanied by a decrease in total REEs. At
576 sites G4 and G6, the dry season LREEs concentrations are lower (Fig. 7d), resulting in declines in the
577 $(Pr/Sm)_{NASC}$ ratios of 0.3 and 0.5 respectively (Table 2). In comparison, the groundwater sites G3, G5,
578 G2, and G10 (Figs. 7e-g) show relatively little temporal variation in both REE patterns and
579 concentrations. For example, both Ce/Ce* and $(Pr/Sm)_{NASC}$ ratios seasonally vary by ≤ 0.2 (Table 2).
580

581 $(Y/Ho)_{NASC}$ ratios are also included in Table 2 because this can act as an indicator of REE sorption due
582 to Yttrium (Y) having a lower affinity for surface-complexes compared with holmium (Ho). Co-
583 precipitation or sorption of REEs to iron oxyhydroxides (e.g. Möller et al., 1998) or particulate matter
584 (e.g. Nozaki et al., 1997) results in the fractionation of Y and Ho. In this study, the $(Y/Ho)_{NASC}$ values
585 (Fig. 7h) are compared with As concentrations. The results show a negative linear correlation
586 (R^2=0.7) between the decreasing $(Y/Ho)_{NASC}$ ratios and increasing As concentrations in both wet and
587 dry season groundwater samples until the groundwater has As concentrations > 100 μg/L. Where
588 groundwater has As concentrations > 100 μg/L the $(Y/Ho)_{NASC}$ ratio increases. The enrichment of
589 $(Y/Ho)_{NASC}$ in groundwater with low As concentrations indicates that the removal of REEs is likely
590 linked to As processes such as sorption or co-precipitation with iron oxyhydroxides.
591
592
593 **5. Discussion**
594
595 **5.1 Hydro(geo)logical processes**
596
597 ***River-groundwater interactions***
598 The hydrochemical results (^3H and EC) from this study did not show much evidence of seasonal-scale
599 recharge of the Bassac River to the shallow aquifer, despite in some areas the measured river depths
600 suggest that this would be possible. Previous studies in other sites of the Cambodian Mekong Delta
601 have highlighted a connection between the Bassac and Mekong River and surrounding shallow
602 aquifers that result in linked changes in groundwater quality (e.g. Polizzotto et al., 2008; Lawson et
603 al., 2016; Richards et al., 2017a, b). Therefore, we hypothesise that the bores sampled in this study
604 were located outside of the zone of influence of recharge from the Bassac River (at distances of 0.3-
605 1 km from the river's edge). Despite the high dry season groundwater pumping rates, the river stable
606 isotope and EC values do indicate potentially dry season inflows to the river from the shallow

aquifer. In addition, the stable isotope results suggest an increase in local delta rainfall contributions to the river during the wet season compared with greater surface water inflows from northern catchments to the river in the dry season. This corresponds with previous work that has used both physical models (MRC, 2009) and stable and radiogenic isotope data (Nguyen et al., 2007).

Groundwater recharge

One groundwater site (G1) showed evidence of local recharge during the wet season by rainfall or inundation waters. This site therefore is located where this is little or no confining unit at the surface. The combination of lower EC, higher REE concentrations and lower stable isotopes in the wet season compared with the dry season highlights an older laterally flowing groundwater system that mixes with wet season recharging rainfall and/or inundation waters. The mixing calculation using $\delta^{18}O$ values highlighted a high percentage (~50 %) of rain/inundation waters that mixed with the groundwater system during the wet season.

A second groundwater site (G7) also showed evidence of recent recharge but, as highlighted by the fractionation of stable isotope values, this is by evaporated waters. At G7, recharge occurs during both the dry and wet season most likely via the nearby permanent surface waters trapped by a dyke in the low elevation areas. Previous studies to the north of the study area have also found ponds and wetlands to be a recharge source for shallow groundwater (e.g. Lawson et al., 2016; Richards et al., 2019). Given the stagnation of these waters at the surface, the underlying sediments must act as a low-infiltration layer. The relatively constant stable isotope and major ion chemistry at G7 suggest that there is constant mixing between the dry and wet season recharge with lateral groundwater flow.

For 7 of the 10 groundwater sites there is no detectable ^{3}H contents, therefore the mean residence times are > 60 years old, and these sites represent shallow groundwater from a semi-confined

633 aquifer at ~30 to 62 m depth. The stable isotope and major ion hydrochemistry also indicates that
634 groundwater from this semi-confined aquifer is not locally or recently recharged by rainfall, river,
635 inundation or irrigation waters and changes in EC are controlled by variations in water-rock
636 interactions in the aquifer and in-aquifer mixing.
637
638
639 **5.2 Seasonal changes in groundwater arsenic concentrations**
640 Simplified schematics for each of the three types of groundwater recharge processes (limited recent
641 recharge, evaporated water and rainfall recharge) are presented in figure 8. At each of the
642 groundwater sites there is dry season groundwater pumping that exceeds wet season pumping. The
643 influence of groundwater pumping versus recharge processes impacting on the As concentrations in
644 groundwater is not consistent between the groundwater sites (Fig. 8) and is explored below.
645
646 ***Model 1. Limited recent recharge***
647 Model 1 is assigned to groundwater sites where the aquifer is semi-confined, there is limited
648 modern recharge ($^{3}H \leq 0.8$ TU), and there is no recharge from evaporated waters or recent rain
649 water. This includes 5 groundwater sites where the seasonal changes in As concentrations are not
650 significant after accounting for total errors (G2, G3, G5, G10 and G4), and 1 groundwater site where
651 there is a dry season increases in the As concentration (by 10.9 μg/L; G6). Further work, including
652 the comparison with groundwater pumping volumes, is required to determine whether the
653 difference in As concentration changes between the sites is related to groundwater pumping
654 practices.
655
656 At G6, the increase in As concentrations correlate with the period of high pumping rates during the
657 dry season. Unlike some As models proposed from sites in Bangladesh, the groundwater pumping at
658 G6 did not induce mixing with younger waters (e.g. Harvey et al., 2002), nor did it induce the dilution

of As concentrations (e.g. Radloff et al., 2017). The groundwater that is drawn into the bore during pumping (during both the dry and wet season) has a mean residence time of > 60 years, and changes in As concentrations are therefore related to seasonal-scale in-aquifer processes that are triggered or accentuated during the relatively high pumping volumes of the dry season.

Groundwater bores installed for water supplies often have long screen intervals to increase the pumping volumes, which is the case for the private bores sampled in this study with screens along the length of the casing. On-going pumping can therefore result in the connection of otherwise separate aquifer zones (Ayotte et al., 2011). At the site G6, changes in As concentrations may result from greater extractions of groundwater during the dry season that draws in groundwater from different aquifer zones that are otherwise not accessed during the wet season when pumping rates are lower. Groundwater elevations have been found to decrease by up to 5 m in the Kandal Province during the June/July irrigation period (JICA, 2002). Since groundwater flows to a bore during pumping are firstly accessed from relatively high hydraulic conductivity (K) zones in the aquifer, only after prolonged pumping will regions of lower K contribute to the groundwater volumes extracted. Therefore, particularly towards the end of the dry season, the continued groundwater pumping can cause inflows of waters with distinct chemical properties. In previous work on the shallow groundwater aquifer in the Mekong Delta, at a site 8 km south of our study area, Wang et al. (2018) reported that the sediments with the highest hydraulic conductivities (K = 3.8×10^{-6} to 4.6×10^{-6} cm/s) were associated with relatively low concentrations of As (11-12 ppm) and total organic carbon (TOC: 0.9-1 wt %), compared with the lower K (2.6×10^{-7} to 5.9×10^{-7} cm/s) sediments that have higher As concentrations (15-28 ppm) and TOC contents (4.8-5.1 wt %). Therefore, pumping-induced inflows from these lower K zones can contribute greater concentrations of As to the groundwater pumped. In comparison, during the wet season, pumped volumes are lower, therefore mostly higher K zones in the aquifer are drawn into the aquifer, thereby reducing the As concentrations.

In addition to mixing processes directly affecting As concentrations during pumping, the resultant groundwater chemistry changes can also potentially induce changes in ion sorption/desorption and mineral dissolution/precipitation processes that also affect As concentrations. For example, in near-neutral waters minor increases in pH can result in desorption processes that increase As concentrations (Richards et al., 2019). However, in this study the increased As concentrations during the dry season is associated with a minor decrease in pH compared with the wet season. Therefore seasonal changes in groundwater pH are not driving changes in As concentrations.

The results from this study highlight that the increase in in-aquifer interactions between groundwater from higher K/lower K zones produces high As concentrations in groundwater in the dry season, which may result from changes in redox-driven processes over short time-frames (McMahon et al., 2011). Reducing groundwater conditions promote the reduction of As(V) to As(III) that can lead to desorption from ferric (Fe(III)) and Mn (hydr)oxides and/or sedimentary organic matter (e.g. Richards et al., 2019). In addition, the release of high OC groundwater can result in the respiration of DOC producing NH_4 and an increase in the reductive dissolution of Fe (hydr)oxides also releasing As into solution (e.g. Lawson et al., 2016). At G6, the changes in groundwater chemistry corresponds with these processes; with dry season increases in Fe concentrations (from 1.23 to 21.57 μg/L), and high concentrations of HCO_3 and NH_4 (Table 1).

Changes in REE patterns and ratios can indicate changes in the groundwater system that are significant for As. For example, temporal changes in REEs in groundwater can result from changes in the aquifer pH and redox conditions and mixing between waters (e.g. Dia et al., 2000; Seto and Akagi, 2008). For model 1, the REE data confirms that sites G3, G5, G2, and G10 (Figs. 7e-g) show relatively little temporal variation in mixing or redox effects on REE patterns and concentrations, similar to low changes in As concentrations. In comparison there are changes in LREEs concentrations and patterns at sites G4 and G6 in the dry season (Fig. 7d), which are likely to result

711 from mixing with waters that have interacted with different mineralogy and/or organic matter
712 compared with wet season groundwater. This is consistent with the As being derived from a low K
713 zone of the aquifer during pumping. However, this change in groundwater mixing during the dry
714 season only results in a significant increase in As concentrations at site G6 and not at site G4 (Fig. 8).
715
716 ***Model 2. Recharge by evaporated surface waters***
717 The second As model is based on data at site G7, where the groundwater has been recently
718 recharged and there is mixing with evaporated waters. At site G7 there is no significant change in As
719 between the dry season (67.6 ±3.6 μg/L) and wet season (64.1 ±3.5 μg/L). Similar to Model 1, this
720 site is located in an area where there are significant increases in groundwater pumping during the
721 dry compared with the wet season. In contrast with model 1, the groundwater from the shallow
722 aquifer is recharged during both the dry and wet seasons by evaporated surface waters. Although
723 recharged by evaporated surface waters, there is no evidence that the As concentrations are high
724 due to affects from evaporation. For example, As molar ratios relative to conservative ions in
725 solution (e.g. Cl) are high at G7 (dry season As/Cl: 0.008) compared to samples with low As
726 concentrations (dry season As/Cl: < 0.00005).
727
728 As concentrations are likely to be controlled by evaporated water recharge processes, and less so by
729 pumping since there are no changes in As concentrations at the seasonal-scale. This is consistent
730 with models proposed in other sites of the Cambodian Mekong Delta where there is limited
731 groundwater pumping, which showed that for groundwater outside of the influence of river inflows,
732 the high As concentrations are predominantly the result of recharge of evaporated surface waters
733 and the transfer of young organic matter into the aquifer resulting in the reductive dissolution of
734 Fe/Mn (hydr)oxides (Lawson et al., 2013, 2016; Richards et al., 2018). The low vertical transfer times
735 (ie. > 200 years; Lawson et al., 2013) of the shallow clay-rich sediments in the Mekong Delta implies

736 that the confining layer underlying the evaporated surface waters at site G7 is relatively thin, and
737 allows for transfer times to the shallow groundwater system of < 60 years (^{3}H data, this study).
738
739 Due to the local recharge processes occurring at site G7, there is less likely to be the horizontal
740 stratification of groundwater chemistry that was proposed in model 1. Increases in dry season
741 groundwater pumping may induce greater drawdown rates of the recharging waters, and may result
742 in the observed increase in the Ce/Ce* ratio (Table 2), which in a reducing aquifer can be indicative
743 of an increase in REEs sourced from an organic-rich environment (Pouret et al., 2010; Davranche et
744 al., 2015). This implies that during the dry season the evaporative water recharge transfers more
745 organic-rich waters compared with the wet season. However, this did not result in a significant
746 increase in As concentrations in the groundwater.
747
748 ***Model 3. Rainfall recharge***
749 Model 3 is based on groundwater at the site G1. This is the only site in this study to show evidence
750 of significant recharge by wet season rainfall, which results in wet season increases in REE
751 concentrations, decreased δ^{18}O and δ^{2}H values, and the dilution of many major ions. Despite this,
752 there were some ion concentrations that increased during recharge, including As (from 1.3 ±0.1 to
753 8.6 ±0.5 μg/L), and Fe (4 to 25 μg/L). Therefore, a driver of increases in As at site G1 is linked to wet
754 season recharge processes, and likely due to the transfers of young OC and the resultant reductive
755 dissolution of Fe(III) (hydr)oxides (as reflected in wet season increases in Fe). Similar to the model 2,
756 due to efficient recharge processes there is unlikely to be any significant horizontal stratification of
757 groundwater chemistry, and the seasonal-scale recharge indicates that at this site there is a clay-
758 window and therefore the shallow aquifer is unconfined.
759
760
761 **5.3 Future work on As models**

As observed in the 3 models proposed, there are multiple physical and biogeochemical processes impacting groundwater in the Kandal region of the Cambodian Mekong Delta that result in the high spatial heterogeneity of the groundwater As concentrations. In contrast, we observe very few sites with significant seasonal changes in groundwater As concentrations. Temporal variations were only observed at two sites, and the causes of these variations ranged from natural processes (significant seasonal recharge at site G1), to potential anthropogenic impacts (from groundwater pumping at site G6). Further work in the region requires an analysis of the seasonal changes in As concentrations at sites such as G6 in combination with groundwater extraction volumes, analysis of sediments, and changes in hydraulic head data. In addition, monitoring bores should be installed so that an analysis of aquifer processes can be undertaken outside of the bias of pumping influences and the regional extent of irrigation pumping effects on groundwater As concentrations can be assessed. This would allow a more in-depth analysis of the natural versus anthropogenic processes controlling the spatial and seasonal changes in As in groundwater from the irrigated area of the Cambodian Mekong Delta. Finally, the on-going projects devoted to rehabilitating current water resources infrastructure (e.g. deepening of the prek channels) raise questions on the potential impact on groundwater quality. The deepening could result in faster vertical transfer times or clay-windows allowing surface water recharge into the semi-confined aquifer, and thus may result in an increase in As mobilisation in groundwater with the introduction of young organic matter.

6. Conclusions

Managing groundwater As contamination issues is important nationally for the rural community of Cambodia in the delta, but also for the 17.5 million Vietnamese people that live down-gradient in the Mekong Delta. This study presents a first insight into the seasonal variations of As concentrations in groundwater in the irrigation region of the Cambodian Mekong Delta. Where the aquifer is semi-confined, this provided ideal sites to consider groundwater pumping impacts on As

concentrations because there were no wet season recharge processes influencing changes in groundwater chemistry. The results from this study show that in the shallow semi-confined aquifer a lack of seasonal variations in As concentrations at most groundwater sites indicates that the wet-dry variations in pumping volumes are not significantly impacting the mobilisation of As in the semi-confined aquifer. There was only one site (G6) that exhibited dry season increases in As concentrations, which is potentially caused by the dry season increases in groundwater pumped for irrigation. In areas where the aquifer is not confined, it was the natural recharge processes (of either evaporated surface waters or wet season rainfall) that controlled As concentrations in groundwater. The results from this study present a conceptual model of the seasonal-scale processes affecting As concentrations in the irrigated area of the Cambodian Mekong Delta, and early findings are similar to other southern and southeast Asia regions such as Bangladesh where models of both natural and anthropogenic processes are required to describe the As processes. In future work, information on pumping volumes is essential to verify (i) whether groundwater extraction is causing the increase in the As concentrations at site G6, and also (ii) whether the lack of seasonal changes in groundwater As concentrations at the other sites of the semi-confined aquifer in the irrigated area is solely controlled by long-term natural processes.

Acknowledgments

The authors wish to acknowledge the help in field translations from Raksmey Phoeurk (Royal University of Agriculture, Phnom Penh), and technical help from colleagues at the Institute of Technology, Cambodia. This study was funded by financial contributions from the Institute for Research and Development, and from the University of Avignon (France).

References

Anderson H.R., 1978. Hydrogeologic Reconnaissance of the Mekong Delta in South Vietnam and Cambodia. U.S. Geological Survey water-supply paper; 1608-R: Contributions to the hydrology of Asia and Oceania. Washington : U.S. Govt. Print. Off.

Anthony E.J., Brunier G., Besset M., Goichot M., Dussouillez P., Nguyen V.L. 2015. Linking rapid erosion of the Mekong River delta to human activities. Scientific Reports, 5:14745, DOI: 10.1038/srep14745.

Aggarwal P.K., Fröhlich K., Kulkarni K.M., and Gourcy L.L. 2004. Stable isotope evidence for moisture sources in the asian summer monsoon under present and past climate regimes, Geophys. Res. Lett., 31, L08203, doi:10.1029/ 2004GL019911.

Ayotte J.D., Szabo Z., Focazio M.J., Eberts S.M. 2011. Effects of human-induced alteration of groundwater flow on concentrations of naturally-occurring trace elements at water-supply wells. Applied Geochemistry 26, 747–762.

Bau, M., 1999. Scavenging of dissolved yttrium and rare earths by precipitating iron oxyhydroxide: experimental evidence for Ce oxidation, Y–Ho fractionation, and lanthanide tetrad effect. Geochimica Cosmochimica Acta 63 (1), 67–77.

Berg M., Trang P.T.K., Stengel C., Buschmann J., Viet P.H., Dan N.V., Giger W., Stuben D. 2008. Hydrological and sedimentary controls leading to arsenic contamination of groundwater in the Hanoi area, Vietnam: The impact of iron-arsenic ratios, peat, river bank deposits, and excessive groundwater abstraction, Chem. Geol., 249, 91–112.

Biddau, R., Cidu, R., Frau, F. 2002. Rare earth elements in waters from albite-bearing granodiorites of central Sardinia, Italy. Chemical Geology, 182, 1–14.

Bravard J-P., Goichot M., Gaillot S. 2013. Geography of Sand and Gravel Mining in the Lower Mekong River. EchoGéo, 26, DOI : 10.4000/echogeo.13659.

Briese E. 1996. Prefeasibility Assessment of the Shallow Groundwater Resources of Cambodia. Asian Development Bank Technical Report TA NO. 2554-CAM: Community Irrigation Rehabilitation Project.

Brunier G., Anthony E.J., Goichot M., Provansal M., Dussouillez P. Recent morphological changes in the Mekong and Bassac river channels, Mekong delta: The marked impact of river-bed mining and implications for delta destabilisation. Geomorphology. Volume 224, 1 November 2014, Pages 177-191.

Clark, I., Fritz, P., 1997. Environmental isotopes in hydrogeology. Lewis Publishers.

Craig H., 1961. Isotopic variations in meteoric waters. Science, 133, 1702–1703.

Davis S.N., Whittemore D.O., Fabryka-Martin J., 1998. Uses of chloride/bromide in studies of potable water. Ground Water 36, 338–351.

Davranche M., Gruau G., Dia A., Marsac R., Pédrot M., Pourret O. 2015. Biogeochemical Factors Affecting Rare Earth Element Distribution in Shallow Wetland Groundwater. Aquatic Geochemistry, 21(2-4), 197–215.

Dia, A., Gruau, G., Olivié-Lauquet, G., Riou, C.,Molénat, J., Curmi, P., 2000. The distribution of rare earth elements in groundwaters: assessing the role of source-rock composition, redox changes and colloidal particles. Geochim. Cosmochim. Acta 64 (24), 4131–4151.

Erban L.E., Gorelick S.M. 2016. Closing the irrigation deficit in Cambodia: Implications for transboundary impacts on groundwater and Mekong River flow. Journal of Hydrology 535, 85–92.

Erban L.E., Gorelick S.M., Zebkerb H.A., Fendorfa S. 2013. Release of arsenic to deep groundwater in the Mekong Delta, Vietnam, linked to pumping-induced land subsidence. PNAS, 110 (34), 13751–13756.

Harvey C.F., Swartz C.H., Badruzzaman A.B.M., KeonBlute N., Yu W., Ali M.A., Jay J., Beckie R., Niedan V., Brabander D., Oates P.M., Ashfaque K.N., Islam S., Hemond H.F., Ahmed M.F. 2002. Arsenic mobility and groundwater extraction in Bangladesh. Science 298 : 1602-1606.

IAEA/WMO. 2019. Global Network of Isotopes in Precipitation. The GNIP Database. Accessible at: https://nucleus.iaea.org/wiser

JICA, 2002. The study on groundwater development in southern Cambodia. Japan International Cooperation Agency (JICA) and Ministry of Rural Development Cambodia, Report. Kokusai Kogyo Co., Ltd., 181p.

Johannesson, K.H., Xiaoping, Z., Caixia, G., Klaus, J.S., Vernon, F.H. 2000. Origin of rare earth element signatures in groundwaters of circumneutral pH from southern Nevada and eastern California, USA. Chemical Geology 164, 239–257.

Jurgens, B.C., McMahon, P.B., Chapelle, F.H., Eberts, S.M., 2009. An Excel® Workbook for Identifying Redox Processes in Ground Water. US Geol. Surv. Open-File Rep. 2009-1004.

Katz B.G., Eberts S.M., Kauffman L.J. 2011. Using Cl/Br ratios and other indicators to assess potential impacts on groundwater quality from septic systems: a review and examples from principal aquifers in the United States. J Hydrol; 397:151–66.

Lawson M., Polya D.A., Boyce A.J., Bryant C., Mondal D., Shantz A., Ballentine C.J.. 2013. Pond-derived organic carbon driving changes in arsenic hazard found in Asian groundwaters. Environ. Sci. Technol., 47, 7085-7094.

Lawson M., Polya D.A., Boyce A.J., Bryant C., Ballentine C.J. 2016. Tracing organic matter composition and distribution and its role on arsenic release in shallow Cambodian groundwaters. Geochimica et Cosmochimica Acta, 178, 160-177.

Le Duy N., Heidbüchel I., Meyer H., Merz B., Apel H. 2017. What controls the stable isotope composition of precipitation in the Asian monsoon region? Hydrol. Earth Syst. Sci., 22, 1239-1262.

Leybourne M.I., and Johannesson K.H. 2008. Rare earth elements (REE) and yttrium in stream waters, stream sediments, and Fe–Mn oxyhydroxides: Fractionation, speciation, and controls over REE + Y patterns in the surface environment. Geochimica et Cosmochimica Acta,72(24), 5962-5983.

Liu C.W., Lin K-H, Kuo Y-M. 2003. Application of factor analysis in the assessment of groundwater quality in a blackfoot disease area in Taiwan. Science of Total Environment, Volume 313, Issues 1–3, 77-89.

Lu, X. X., Kummu M., Oeurng C. 2014. Reappraisal of sediment dynamics in the Lower Mekong River, Cambodia, Earth Surface Processes and Landforms, 39(14), 1855-1865.

Mailloux B.J., Trembath-Reichert E., Cheung J., Watson M., Stute M., Freyer G.A., Ferguson A.S. , Ahmed K.M., Alam M.J., Buchholz B.A., Thomas J., Layton A., Zheng Y., Bostick B., van Geen, A. 2013. Advection of surface-derived organic carbon fuels microbial reduction in Bangladesh groundwater. PNAS 110 (13), 5331–5335.

Mekong River Commission, 2019. MRC website, Hydrological Stations: http://ffw.mrcmekong.org/stations.php?StCode=LUA&StName=Luang%20Prabang

McMahon P.B., Chapelle F.H., Bradley P.M. 2011. Evolution of Redox Processes in Groundwater. Ch. 26 In Aquatic Redox Chemistry; Tratnyek, P., et al.; ACS Symposium Series; American Chemical Society: Washington, DC, 2011. 581-597

Möller, P., Dulski, P., Gerstenberger, H., Morteani, G., Fuganti, A. 1998. Rare earth elements, yttrium and H, O, C, Sr, Nd and Pb isotope studies in mineral waters and corresponding rocks from NW-Bohemia, Czech Republic. Applied Geochemistry, 13 (8), 975–994.

MRC, 2009. The Flow of the Mekong. Mekong River Commission (MRC) Management Information booklet series No. 2, Printed by the MRC Secretariat, Series editor Dr Tim Burnhill, Mekong River Commission, 12p.

Murphy T., Phan K., Yumvihoze E., Irvine K., Wilson K., Lean D., Poulain A., Laird B., Hing Man Chan L. 2018. Effects of Arsenic, Iron and Fertilizers in Soil on Rice in Cambodia. Journal of Health & Pollution Vol. 8, No. 19, 1-12.

Murphy T., Phan K., Chan L., Poulain A., Irvine K.N., Lean D. 2017. Appendix 2 Effect of Irrigation Water on Arsenic Content of Rice. In: Innovative solutions for food security/safety issues

caused by arsenic contamination of rice in Cambodia. Final Technical Report. IDRC Project No: 107718-00020799-032.
Neumann R.B., Ashfaque K.N, Badruzzaman A.B.M., Ali M.A., Shoemaker J.K., Harvey C.F. 2010. Anthropogenic influences on groundwater arsenic concentrations in Bangladesh. Nat. Geosci. 3 (1), 46–52.
Nguyen K.C., Huynh L., Le D.C., Nguyen V.N., Tran B.L. 2007. Isotope Composition of Mekong River flow water in the south of Vietnam. Advances in isotope hydrology and its role in sustainable water resources management (IHS-2007). Proceedings of a symposium. Vol. 2, 197-209.
Nozaki, Y., Zhang, J., Amakawa, H., 1997. The fractionation between Y and Ho in the marine environment. Earth and Planetary Science Letters, 148, 329–340.
Parkhurst D.L., Appelo C.A.J. 1999. User's Guide to PHREEQC (Version 2): a Computer Program for Speciation, Batch-reaction, One-dimensional Transport, and Inverse Geochemical Calculations, Water-resources Investigations Report.
Papacostas N.C, Bostick B.C, Quicksall A.N., Landis J.D., Sampson M. 2008. Geomorphic controls on groundwater arsenic distribution in the Mekong River Delta, Cambodia. Geology, 36 (11): 891–894.
Pederick R. L., Gault A. G., Charnock J. M., Polya D. A., Lloyd J. R. 2007. Probing the biogeochemistry of arsenic: Response of two contrasting aquifer sediments from Cambodia to stimulation by arsenate and ferric iron. Journal of Environmental Science and Health, Part A, 42, 1763- 1774.
Phan K., Phan S., Huoy L., Suy B., Hung Wong M., Hisham Hashim J., Salleh Mohamed Yasin M., Mohamed Aljunid S., Sthiannopkao S., Kim K-W. 2013. Assessing mixed trace elements in groundwater and their health risk of residents living in the Mekong River basin of Cambodia. Environmental Pollution 182, 111-119.
Pillot, D. (2007). Jardins et Rizières au Cambodge : enjeux du développement durable. Paris: KARTHALA Editions.
Polizzotto M.L., Kocar B.D., Benner S.G., Sampson M., Fendorf S. 2008. Near-surface wetland sediments as a source of arsenic release to ground water in Asia. Nature 454, 505–508.
Polya D., Gault A., Diebe N., Feldman P., Rosenboom J.W., Gilligan, E., Fredericks D., Milton A., Sampson M., Rowland H., Lythgoe P., Jones J., Middleton C., Cooke D. (2005). Arsenic hazard in shallow Cambodian groundwaters. Mineralogical Magazine, 69(5), pp. 807-823.
Pourret O., Davranche M., Gruau G., Dia A. 2007. Rare earth elements complexation with humic acid. Chemical Geology 243, 128-141.
Pourret O., Gruau G., Dia A., Davranche M., and Molénat J. 2010 Colloidal control on the distribution of rare earth elements in shallow groundwaters. Aquatic Geochemistry 16 (1), 31-59.
Quicksall B., Bostick C., Sampson M.L. 2008. Linking organic matter deposition and iron mineral transformations to groundwater arsenic levels in the Mekong delta, Cambodia. Applied Geochemistry. Volume 23, Issue 11, Pages 3088-3098.
Radloff K.A., Zheng Y., Stute M., Weinman B., Bostick B., Mihajlov I., Bounds M., Rahman M.M., Huq M.R., Ahmed K.M., Schlosser P., van Geen A. 2017. Reversible adsorption and flushing of arsenic in a shallow, Holocene aquifer of Bangladesh. Appl. Geochem. 77, 142–157.
Raessler M. 2018. The Arsenic Contamination of Drinking and Groundwaters in Bangladesh: Featuring Biogeochemical Aspects and Implications on Public Health. Arch Environ Contam Toxicol., 75(1): 1–7.
Rasmussen W.C., Bradford G.M. 1977. Groundwater Resources of Cambodia. U.S. Geological Survey water-supply paper; 1608-P: Contributions to the hydrology of Asia and Oceania. Washington : U.S. Govt. Print. Off.
Richards, L.A., Magnone D., Sovann C., Kong C., Uhlemann S., Kuras O., van Dongen B.E., Ballentine C.J., Polya D.A. 2017a. High resolution profile of inorganic aqueous geochemistry and key redox zones in an arsenic bearing aquifer in Cambodia. Sci. Total Environ.590–591, 540–553.

Richards L.A., Sültenfuß J., Ballentine C.J., Magnone D., van Dongen B.E., Sovann C., Polya D.A. 2017b. Tritium Tracers of Rapid Surface Water Ingression into Arsenic-Bearing Aquifers in the Lower Mekong Basin, Cambodia. Procedia Earth and Planetary Science 17, 845-848.

Richards L.A., Magnone D., Boyce A.J., Casanueva-Marenco M.J., van Dongen B.E., Ballentine C.J., Polya D.A. 2018. Delineating sources of groundwater recharge in an arsenic-affected Holocene aquifer in Cambodia using stable-isotope based mixing models. Journal of Hydrology 557, 321-334.

Richards L.A., Magnone D., Sültenfuß J., Chambers L., Bryant C., Boyce A.J., van Dongen B.E., Ballentine C.J., Sovann C., Uhlemann S., Kuras O., Gooddy D.C., Polya D.A. 2019. Dual in-aquifer and near surface processes drive arsenic mobilization in Cambodian groundwaters. Science of the Total Environment 659, 699–714.

Richards L., Casanueva-Marenco M.J., Magnone D., Sovann C., van Dongen B.E., Polya D.A. 2019 Contrasting sorption behaviours affecting groundwater arsenic concentration in Kandal Province, Cambodia. Geoscience Frontiers, 10 (5), 1701-1713.

Rowland H.A.L., Pederick R.L., Polya D.A., Pancost R.D., Van Dongen B.E., Gault A.G., Vaughan D.J., Bryant C., Anderson B., Lloyd J.R. 2007. The control of organic matter on microbially mediated iron reduction and arsenic release in shallow alluvial aquifers, Cambodia. Geobiology. 5, 281-292.

SCP (2018) Water resources management and agro-ecological transition for Cambodia. WAT4CAM program phase 1 - project feasibility report, 120p.

Seto M., Akagi T. 2008. Chemical condition for the appearance of a negative Ce anomaly in stream waters and groundwaters. Geochemical Journal, Vol. 42, pp. 371 to 380.

Smith R., Knight R., Fendorf S. 2018. Overpumping leads to California groundwater arsenic threat. Nature Communications 9 (2089), 1-6.

SOFRECO (2019). Final report, Water & Agricultural Sector Programme (WASP)-Package 2; Technical Assistance for the implementation of Preks of Kandal Component (TA Preks). Report to the Ministry of Water and Meteorology. Phnom Penh: Cambodia.

van Dongen B.E., Rowland H.A.L., Gault A.G., Polya D.A., Bryant C., Pancost R.D. 2008. Hopane, sterane and n-alkane distributions in shallow sediments hosting high arsenic groundwaters in Cambodia. Appl. Geochem. 23, 3047–3058

Wang Y., Le Pape P., Morin G., Asta M.P., King G., Bártová B., Suvorova E., Frutschi M., Ikogou M., Hoai Cong Pham V., Le Vo P., Herman F., Charlet L., Bernier-Latmani R. 2018. Arsenic Speciation in Mekong Delta Sediments Depends on Their Depositional Environment. Environ. Sci. Technol. 2018, 52, 3431−3439.

WHO, 2017. Guidelines for drinking-water quality: fourth edition incorporating the first addendum. ISBN 978-92-4-154995-0, p 631**.**

WSP, 2019. Arsenic Contamination by Well. Ministry of Rural Development of Cambodia and Water and sanitation program (WSP) of the World Bank. The online well database of Cambodia. Accessed from: https://cambodiawellmap.com/worldbank/maps.

WSP, 2019. Water sanitation program database, Ministry of water resources and meteorology https://cambodiawellmap.com/worldbank/maps/44788/well-summary-tool.

Yeghicheyan D., Bossy C., Bouhnik Le Coz M., Heimburger A., Lacan F., Lanzanova A., Rousseau T., Seidel J.L., Tharaud M., Douchet C., Candaudap F., Chmeleff J., Cloquet C., Delpoux S., Labatut M., Losno R., Pradoux C., Sivry Y., Sonke J. 2013. A compilation of Silicon, Rare Earth Elements and twenty other trace elements measured in the natural river water standard SLRS-5. Geostandard and Geoanalytical Research, 37, 4, 449-467, doi 11.111/j.1751-908X2013.00232.x.

Yeghicheyan D., Aubert D., Bouhnik-Le Coz M., Chmeleff J., Delpoux S., Djouraev I., Granier G., Lacan F., Piro J-L., Rousseau T., Cloquet C., Marquet A., Menniti C., Pradoux C., Freydier R., Vieira da Silva-Filho E., Suchorski K. 2019. New Interlaboratory Characterisation of Silicon, Rare Earth Elements and Twenty-Two other Trace Element Mass Fractions in the Natural River Water

Certified Reference Material SLRS-6 (NRC-CNRC). Geostandards and Geoanalytical Research, 43(3), 475-496. DOI: 10.1111/ggr.12268.

Table 1

Click here to download Table: Table 1.docx

Table 1. Field parameters, major ions, stable and radiogenic isotope results for the Bassac River, inundation and irrigation water, and groundwater in the dry and wet seasons (2017 and 2018).

Sample ID	Date	Depth (m)	pH	EC (µs/cm)	HCO_3 mg/L	Cl	F	Br	PO_4	NO_2	NO_3	NH_4	SO_4	Na	K	Mg	Ca	SiO_2	$\delta^{18}O$ ‰ VSMOW	$\delta^{2}H$ ‰ VSMOW	^{3}H TU	± (TU)	Evaporation[a] %	Cl/Br molar ratio
Bassac River																								
R1	13-Jun-18		7.71	209	70.8	12.2	0.06	<0.01	<0.01	< 2	< 2	< 2	14.1	9.8	2.3	5.5	19.7	5.0	-7.9	-55.3	2.6	0.3		
	26-Sep-18		7.84	112	53.7	3.8	0.05	<0.01	<0.01	< 2	< 2	< 2	2.4	3.8	1.9	2.7	12.2	5.1	-7.3	-50.4	1.8	0.3		
R2	13-Jun-18		7.75	207	78.1	12.4	0.05	<0.01	<0.01	< 2	< 2	< 2	14.2	9.9	2.4	5.7	19.9	4.9	-7.8	-55.2	n.a.			
R3	13-Jun-18		7.73	207	76.9	12.9	0.05	<0.01	<0.01	< 2	< 2	< 2	14.0	10.1	2.5	5.6	19.7	5.0	-7.9	-55.1	2.9	0.4		
	26-Sep-18		7.82	112	53.7	3.5	0.06	<0.01	<0.01	< 2	< 2	< 2	2.4	3.8	1.8	2.6	12.2	5.0	-7.3	-50.4	2.5	0.3		
R4	13-Jun-18		7.68	206	78.1	12.3	0.03	<0.01	<0.01	< 2	< 2	< 2	13.9	10.1	2.4	5.6	19.2	5.0	-7.8	-54.9	n.a.			
R5	13-Jun-18		7.73	206	78.1	12.7	0.02	<0.01	<0.01	< 2	< 2	< 2	13.9	10.5	2.8	5.6	19.6	4.8	-7.8	-54.9	2.4	0.6		
	26-Sep-18		7.79	109	52.5	3.6	0.02	<0.01	<0.01	< 2	< 2	< 2	2.7	4.0	1.5	2.7	12.3	5.0	-7.3	-50.5	2.2	0.5		
R6	13-Jun-18		7.68	206	75.6	12.2	0.01	<0.01	<0.01	< 2	< 2	< 2	14.0	9.9	2.3	5.6	19.6	4.9	-7.8	-54.7	3.0	0.3		
R7	13-Jun-18		7.68	204	74.4	12.1	0.02	<0.01	<0.01	< 2	< 2	< 2	13.5	9.8	2.2	5.5	17.8	5.0	-7.8	-54.4	2.3	0.3		
	26-Sep-18		7.43	110	54.9	4.1	0.02	<0.01	<0.01	< 2	< 2	< 2	2.8	4.0	2.5	2.8	12.7	4.9	-7.3	-50.6	1.8	0.4		
R8	13-Jun-18		7.70	201	74.4	12.1	<0.01	<0.01	<0.01	< 2	< 2	< 2	13.1	9.7	2.3	5.3	21.1	4.9	-7.8	-54.4	n.a.			
R9	13-Jun-18		7.70	199	73.2	11.8	<0.01	<0.01	<0.01	< 2	< 2	< 2	13.0	9.6	2.2	5.6	18.7	4.9	-7.8	-54.2	n.a.			
R10	13-Jun-18		7.70	197	70.8	11.6	0.00	<0.01	<0.01	< 2	< 2	< 2	13.1	9.7	2.1	5.5	18.9	5.5	-7.7	-53.8	2.4	0.5		
	26-Sep-18		7.70	110	57.3	3.9	0.02	<0.01	<0.01	< 2	< 2	< 2	2.5	4.0	1.8	2.8	12.7	4.9	-7.3	-50.9	1.9	0.4		
R2b	19-Jun-17		n.a.	159	53.7	11.5	0.04	0.02	<0.01	< 2	< 2	9	<0.01	8.9	2.2	4.2	14.5	n.a.	-7.7	-55.1	n.a.			1375
R8b	27-Sep-17		n.a.	113	56.4	3.5	0.03	<0.01	<0.01	< 2	< 2	4	<0.01	3.4	1.2	2.8	11.9	n.a.	-9.5	-68.3	n.a.			
Irrigation/drainage water																								
1	15-Jun-17		n.a.	319	151.3	41.1	0.27	0.10	0.12	< 2	5	38	0.1	18.0	5.9	13.0	30.7	n.a.	-5.0	-36.0	n.a.			906
2	19-Jun-17		n.a.	460	104.9	20.1	0.23	0.07	<0.01	< 2	< 2	15	<0.01	24.2	3.2	9.9	29.6	n.a.	-4.3	-36.4	n.a.			628
4	19-Jun-17		n.a.	301	44.4	34.5	0.08	0.09	<0.01	< 2	< 2	25	<0.01	31.6	7.5	8.8	13.1	n.a.	-0.8	-18.4	n.a.			826
5	19-Jun-17		n.a.	228	54.9	16.5	0.07	0.06	0.01	17	2	13	0.01	6.4	5.8	7.3	16.5	n.a.	-5.6	-42.3	n.a.			662
6	19-Jun-17		n.a.	286	88.6	19.7	0.08	0.06	<0.01	< 2	< 2	16	<0.01	24.5	4.2	8.6	25.1	n.a.	-4.0	-34.4	n.a.			782
7	19-Jun-17		n.a.	175	61.0	12.2	0.05	0.03	<0.01	< 2	< 2	10	<0.01	11.2	2.4	4.8	16.0	n.a.	-6.9	-51.1	n.a.			947
Floodwater																								
SK2	27-Sep-17		n.a.	203	60.4	4.6	0.09	<0.01	<0.01	< 2	< 2	6	<0.01	2.9	1.6	3.4	12.3	n.a.	-8.3	-61.6	n.a.			
SK1	27-Sep-17		n.a.	113	83.2	12.6	0.04	<0.01	<0.01	< 2	< 2	16	<0.01	17.7	2.2	5.6	19.4	n.a.	-8.8	-64.7	n.a.			
Groundwater																								
G1	14-Jun-18	38	7.1	592	290.4	18.9	0.64	0.13	<0.01	< 2	< 2	< 2	27.2	50.3	2.2	24.9	39.6	20.3	-7.9	-55.1	≤ 0.7		28	340
	26-Sep-18		7.2	86	40.3	4.6	0.05	<0.01	0.86	< 2	< 2	< 2	2.5	2.7	7.0	2.6	5.7	8.0	-9.1	-58.8	0.8	0.3	16-21	
G2	14-Jun-18	34	7.0	481	283.0	10.8	0.73	0.39	<0.01	< 2	< 2	< 2	0.3	69.1	2.0	14.1	18.9	18.5	-8.2	-57.1	≤ 0.6		24	62
	26-Sep-18		7.4	546	319.6	11.7	0.40	<0.01	<0.01	< 2	< 2	< 2	2.0	60.6	2.4	19.8	30.1	20.5	-8.0	-56.1	≤ 0.6		26	
G3	14-Jun-18	62	6.9	4110	402.6	1121.3	0.93	3.39	<0.01	< 2	< 2	< 2	5.2	672.5	3.1	69.6	81.0	29.4	-8.2	-57.5	≤ 0.6		24	746
	26-Sep-18		7.1	4220	408.7	1234.5	0.61	4.00	<0.01	< 2	< 2	< 2	1.2	671.0	4.3	61.0	85.0	28.9	-8.2	-57.7	≤ 0.5		23-24	695
G4	14-Jun-18	35	7.7	463	268.4	8.1	0.05	<0.01	0.88	< 2	< 2	8	<0.01	31.9	4.4	13.1	35.2	15.6	-8.0	-55.7	≤ 0.8		26-27	
	26-Sep-18		7.9	460	264.7	6.4	0.10	<0.01	1.21	< 2	< 2	9	<0.01	31.7	5.7	12.8	33.3	16.3	-8.0	-55.7	≤ 0.5		26-27	
G5	14-Jun-18	38	7.5	698	359.9	25.3	0.03	<0.01	<0.01	< 2	< 2	20	<0.01	31.2	4.6	23.6	46.9	9.0	-8.0	-56.7	≤ 0.5		25-26	
	26-Sep-18		7.7	748	375.8	34.7	0.06	0.17	<0.01	< 2	< 2	23	<0.01	36.1	6.3	24.2	45.8	8.1	-8.0	-56.5	≤ 0.5		25-27	464
G6	14-Jun-18	40	7.1	815	268.4	113.1	0.52	<0.01	<0.01	< 2	< 2	8	0.3	103.3	3.2	18.8	24.6	7.8	-8.6	-59.6	≤ 0.3		19-21	
	26-Sep-18		7.3	589	297.7	30.8	0.41	0.12	<0.01	< 2	< 2	9	<0.01	56.0	4.2	19.3	26.0	15.1	-8.6	-59.6	≤ 0.7		19-20	592
G7	14-Jun-18	18	6.9	284	133.0	4.2	<0.01	<0.01	<0.01	< 2	< 2	< 2	<0.01	10.3	0.8	7.0	24.9	18.6	-4.1	-33.4	1.2	0.3	66-71	
	26-Sep-18		7.2	293	144.0	4.3	0.14	<0.01	<0.01	< 2	< 2	2	<0.01	11.0	1.9	7.2	25.1	20.3	-4.3	-34.4	0.8	0.4	65-69	
G8	14-Jun-18	22	6.8	248	115.9	4.4	<0.01	<0.01	<0.01	< 2	< 2	< 2	3.0	10.7	1.0	6.2	22.2	19.2	-3.5	-28.7	1.2	0.4	73-80	
G9	14-Jun-18	35	7.4	456	263.5	13.0	0.38	<0.01	<0.01	< 2	< 2	< 2	1.5	25.3	1.5	27.5	31.0	19.2	-8.0	-55.8	≤ 0.5		26-27	
	26-Sep-18		7.5	412	242.8	9.9	0.44	<0.01	<0.01	< 2	< 2	< 2	0.6	18.9	1.9	27.0	25.4	19.8	-8.2	-56.3	≤ 0.5		25-26	
G10	14-Jun-18	25	7.3	1214	269.6	19.1	0.50	<0.01	<0.01	< 2	< 2	< 2	472.8	96.5	0.8	56.5	88.6	21.0	-7.6	-53.0	≤ 0.4		31-32	
	26-Sep-18		7.5	1207	295.2	21.5	0.67	0.14	<0.01	< 2	< 2	< 2	457.3	100.1	1.5	55.6	92.4	20.1	-7.6	-53.1	≤ 0.8		30-32	347

a: Evaporation values represent the modelled % of groundwater sourced from evaporated water (Richards et al., 2018); n.a.: not analysed.

Table 2

Click here to download Table: Table 2.docx

Table 2. Trace element and rare earth element concentrations and ratios for the Bassac River and groundwater in the dry and wet seasons (2018).

Sample ID	Date	As	sample error	[a]total error	Li	B	Al	Mn	Fe	Rb	Sr	Ba	Pb	Y	La	Ce	Pr	Nd	Sm	Eu	Gd	Tb	Dy	Ho	Er	Tm	Yb	Lu	$(Yb/Nd)_{NASC}$	[b]Ce/Ce*	$(Y/Ho)_{NASC}$	$(Pr/Sm)_{NASC}$
Bassac River		µg/L	±	±	µg/L									ng/L																			
R1	13-juin-18	1.4	0.0	0.1	2.2	18.0	11.2	0.3	11.5	3.8	126.5	40.4	0.0	28.6	17.9	29.2	6.2	24.2	4.8	1.2	5.3	0.8	4.3	0.9	2.5	0.4	2.4	0.4	1.1	0.6	0.9	0.9
	26-sept-18	1.3	0.0	0.1	0.6	6.1	7.8	16.2	11.6	1.8	55.5	31.4	0.0	18.8	13.0	23.1	3.6	18.1	3.6	0.9	4.1	0.6	3.3	0.7	1.8	0.3	1.7	0.3	1.0	0.7	1.2	0.7
R2	13-juin-18	1.4	0.0	0.1	2.3	18.4	9.4	0.3	9.4	3.9	127.9	40.3	0.0	23.6	14.7	23.6	4.3	16.2	3.7	1.1	4.1	0.6	3.6	0.8	2.3	0.4	2.1	0.3	1.4	0.6	0.9	0.8
R3	13-juin-18	1.4	0.0	0.1	2.2	18.0	6.7	0.3	6.3	4.1	128.8	39.5	0.0	20.6	12.8	18.3	3.5	14.3	3.6	1.1	3.6	0.5	3.0	0.6	1.9	0.3	2.0	0.3	1.5	0.6	1.0	0.7
	26-sept-18	0.9	0.0	0.1	0.7	5.7	5.8	3.5	17.0	1.6	54.2	26.4	0.0	23.8	18.6	34.1	5.3	23.4	5.5	1.3	5.4	0.7	4.3	0.8	2.4	0.3	2.1	0.3	0.9	0.7	0.9	0.7
R4	13-juin-18	1.4	0.0	0.1	2.3	18.1	12.5	0.3	13.4	3.7	127.5	39.5	0.0	29.1	20.2	33.6	5.4	25.0	4.9	1.1	5.0	0.8	5.0	0.9	2.6	0.4	2.6	0.4	1.1	0.7	1.0	0.8
R5	13-juin-18	1.5	0.0	0.1	2.3	18.3	14.4	1.8	16.5	3.9	126.9	39.7	0.1	66.0	26.2	46.5	7.5	35.9	8.9	2.1	11.2	1.6	10.2	1.8	5.3	0.7	4.3	0.6	1.3	0.7	1.1	0.6
	26-sept-18	0.8	0.0	0.0	0.6	5.7	6.3	1.5	12.4	1.8	54.4	31.6	0.0	28.8	18.6	27.2	4.9	21.6	5.1	1.3	5.5	0.7	4.3	0.9	2.5	0.3	2.1	0.4	1.0	0.6	1.0	0.7
R6	13-juin-18	1.4	0.0	0.1	2.2	17.9	9.5	0.3	9.5	3.6	127.4	38.2	0.0	23.3	16.0	26.0	4.0	17.4	4.0	0.9	4.1	0.6	3.7	0.7	2.1	0.3	2.2	0.3	1.4	0.7	1.0	0.7
R7	13-juin-18	1.4	0.0	0.1	2.3	17.6	10.7	0.3	11.1	3.6	126.3	38.6	0.0	25.9	17.2	28.3	4.4	20.2	4.4	1.0	4.9	0.7	4.2	0.8	2.3	0.4	2.1	0.3	1.1	0.7	0.9	0.7
	26-sept-18	0.8	0.0	0.0	0.5	5.5	5.0	1.2	11.5	1.7	53.7	32.5	0.0	25.1	16.9	25.1	4.4	20.2	4.7	1.1	4.7	0.7	3.8	0.7	2.3	0.3	1.9	0.3	1.0	0.6	1.0	0.7
R8	13-juin-18	1.3	0.0	0.1	2.2	17.6	11.7	0.3	12.2	3.5	125.4	37.6	0.0	25.7	19.1	30.6	4.7	21.2	5.0	1.2	4.9	0.7	4.0	0.8	2.6	0.3	2.2	0.3	1.1	0.7	1.0	0.7
R9	13-juin-18	1.3	0.0	0.1	2.2	17.1	11.0	0.3	11.3	3.4	123.3	36.3	0.0	25.5	18.4	30.1	4.8	21.1	5.0	1.2	5.1	0.6	4.4	0.8	2.5	0.3	2.4	0.3	1.2	0.7	0.9	0.7
R10	13-juin-18	1.3	0.0	0.1	2.2	17.7	30.5	0.5	31.4	3.6	127.6	38.4	0.0	44.4	38.8	69.9	9.9	44.8	10.3	2.3	9.1	1.3	7.9	1.5	4.3	0.6	3.8	0.6	0.9	0.8	0.9	0.7
	26-sept-18	0.7	0.0	0.0	0.5	5.7	6.7	0.8	13.7	1.7	53.4	29.1	0.0	27.3	19.2	29.1	5.1	22.8	5.5	1.4	5.6	0.8	4.3	0.8	2.4	0.4	2.1	0.4	1.0	0.6	0.7	0.7
Groundwater																																
G1	14-juin-18	1.3	0.0	0.1	9.4	34.1	1.5	485.2	3.9	0.3	418.8	180.9	0.1	15.8	3.8	4.4	0.6	2.4	0.8	0.2	0.8	0.1	1.0	0.2	0.9	0.1	0.8	0.1	3.7	0.7	1.9	0.5
	26-sept-18	8.6	0.0	0.5	2.3	13.0	18.4	109.9	25.2	2.9	43.3	31.2	0.2	46.8	28.8	67.1	8.2	35.3	8.8	2.3	9.7	1.3	7.7	1.6	4.8	0.6	4.3	0.6	1.3	1.0	0.9	0.7
G2	14-juin-18	0.6	0.0	0.0	16.4	41.6	1.4	891.6	1.7	0.6	129.3	72.7	0.2	15.7	2.0	3.4	0.3	1.5	0.6	0.2	0.6	0.1	0.9	0.3	1.2	0.2	1.0	0.2	7.3	0.9	1.6	0.4
	26-sept-18	0.5	0.0	0.0	19.6	31.4	8.7	788.1	1.4	0.6	183.8	77.7	0.1	9.5	1.8	2.2	0.2	2.3	0.5	0.1	0.5	0.1	0.4	0.1	0.5	0.1	0.6	0.1	2.8	0.7	2.5	0.4
G3	14-juin-18	0.2	0.0	0.0	96.2	169.3	1.7	1696.1	<0.03	0.3	669.4	189.1	0.1	22.2	2.8	3.2	0.4	1.5	0.8	0.3	1.5	0.2	1.5	0.3	1.0	0.2	1.4	0.2	9.8	0.7	2.2	0.3
	26-sept-18	0.2	0.0	0.0	87.1	164.6	3.4	1609.8	3.9	0.6	678.4	172.4	0.0	18.0	3.0	2.6	0.4	2.0	0.6	0.2	0.9	0.1	0.7	0.2	0.7	0.1	0.7	0.1	3.9	0.5	3.2	0.5
G4	14-juin-18	231.9	2.1	12.5	4.6	105.0	1.8	213.8	8.0	14.4	784.1	1004.6	0.0	2.2	4.8	0.7	0.0	0.3	0.6	0.2	<0.02	<0.05	<0.11	<0.02	<0.10	0.0	<0.08	0.0		0.4		0.0
	26-sept-18	218.5	1.5	11.7	4.5	103.9	18.3	209.4	6.5	14.0	725.2	886.5	0.0	6.4	8.7	4.8	0.7	5.7	1.5	0.3	1.0	0.1	0.7	0.1	0.4	0.1	0.5	0.1	0.8	0.4	2.0	0.3
G5	14-juin-18	383.7	10.7	23.0	4.6	73.4	1.1	1035.8	5.9	7.3	496.0	1657.0	0.0	2.8	15.8	0.7	0.3	1.7	2.1	0.5	<0.02	<0.05	<0.11	0.0	<0.10	<0.01	<0.08	<0.01		0.1	1.7	0.1
	26-sept-18	393.8	2.0	21.0	4.8	79.8	2.3	1115.9	3.3	6.8	471.7	1756.1	0.0	2.9	3.1	1.9	0.5	3.9	1.5	0.4	1.3	0.1	0.8	0.1	0.2	0.0	0.2	0.1	0.7	0.3	1.0	0.2
G6	14-juin-18	14.6	0.3	0.8	6.3	54.4	0.7	885.8	21.6	1.8	246.7	138.2	0.0	1.6	1.4	0.8	0.1	0.4	0.3	0.2	<0.02	<0.05	<0.11	<0.02	0.1	<0.01	<0.08	0.1		0.6		0.1
	26-sept-18	2.7	0.1	0.2	6.3	47.3	1.9	938.4	1.2	1.7	239.6	77.5	0.0	6.9	3.3	3.7	0.6	2.7	0.7	0.2	0.8	0.1	0.5	0.1	0.4	0.1	0.3	0.1	1.3	0.6	1.6	0.6
G7	14-juin-18	67.6	0.3	3.6	3.8	16.2	0.2	450.7	657.4	2.4	145.1	383.1	0.0	0.9	9.7	15.3	2.2	9.7	2.1	0.6	2.4	0.2	1.5	0.3	0.9	0.2	1.0	0.1	1.1	0.7	0.1	0.8
	26-sept-18	64.1	0.8	3.5	3.2	17.1	0.5	392.1	8.6	3.8	136.6	334.8	0.0	1.6	2.5	1.7	0.9	3.5	0.9	0.2	0.8	0.1	0.5	0.1	0.3	0.0	0.3	0.1	1.0	0.2	0.5	0.7
G8	14-juin-18	106.1	1.1	5.7	2.6	16.0	0.1	608.2	5095.0	3.1	121.9	200.6	0.0	0.8	1.8	<0.42	<0.01	0.2	0.5	0.4	<0.02	<0.05	<0.11	<0.02	<0.10	<0.01	<0.08	<0.01				
G9	14-juin-18	1.1	0.1	0.1	19.2	25.8	0.7	267.1	15.8	0.2	220.5	29.4	0.0	33.7	3.6	8.0	0.8	4.2	1.0	0.4	1.6	0.2	1.9	0.4	1.5	0.2	1.0	0.2	2.6	1.0	2.3	0.6
	26-sept-18	1.4	0.1	0.1	17.3	24.7	1.2	296.4	3.1	0.6	177.8	24.9	0.0	4.1	1.1	1.1	0.2	0.9	0.3	0.1	0.5	0.1	0.3	0.1	0.2	0.0	0.1	0.0	1.6	0.5	2.1	0.4
G10	14-juin-18	1.2	0.0	0.1	30.2	35.7	1.1	835.1	9.2	0.5	759.5	30.9	0.3	39.9	3.0	5.0	0.6	2.7	0.7	0.2	1.3	0.2	2.0	0.5	1.5	0.2	1.3	0.2	5.3	0.8	2.5	0.6
	26-sept-18	0.9	0.1	0.1	28.1	34.3	4.5	1050.3	3.2	0.6	686.5	27.9	0.0	47.2	7.7	9.1	1.0	4.3	1.2	0.4	1.9	0.3	3.1	0.7	2.6	0.3	2.1	0.2	5.1	0.7	2.0	0.6

a: $\sqrt{(\text{sample error}^2 + \text{analytical error}^2)}$; b: $Ce/Ce^* = Ce_{NASC} / (La_{NASC}/Pr_{NASC})^{0.5}$

Table 3

Click here to download Table: Table 3.docx

Table 3. SLRS-6 data from this study, and CRM SLRS-6 data from Yeghicheyan et al. (2019) and certified values.

Element	SLRS-6 (n=6)[a]	2 σ STD	CRM SLRS-6
	µg/L	%	µg/L
Li	0.53 ± 0.04	6.7%	0.53 ± 0.02
B	7.33 ± 0.34	4.6%	7.39 ± 1.28
Al	33.7 ± 0.9	2.7%	33.8 ± 2.2[c]
Mn	2.16 ± 0.07	3.2%	2.12 ± 0.1[c]
Fe	82.8 ± 1.6	1.9%	84.3 ± 3.6[c]
As	0.57 ± 0.03	5.3%	0.57 ± 0.08[c]
Rb	1.50 ± 0.05	3.3%	1.41 ± 0.05
Sr	41.21 ± 0.68	1.7%	40.66 ± 0.32[c]
Ba	14.3 ± 0.64	4.5%	14.28 ± 0.48[c]
Pb	0.169 ± 0.009	5.3%	0.17 ± 0.026[c]
Y	0.133 ± 0.003	2.3%	0.128 ± 0.006
La	0.249 ± 0.004	1.6%	0.248 ± 0.012
Ce	0.295 ± 0.011	3.7%	0.293 ± 0.015
Pr	0.061 ± 0.012	11.7%	0.059 ± 0.002
Nd	0.238 ± 0.002	4.2%	0.228 ± 0.009
Sm	0.041 ± 0.002	4.9%	0.039 ± 0.002
Eu	0.008 ± 0.001	6.0%	0.007 ± 0.001
Gd	0.033 ± 0.001	3.0%	0.032 ± 0.002
Tb	0.004 ± 0.001	9.3%	0.004 ± 0.001
Dy	0.023 ± 0.001	3.3%	0.022 ± 0.001
Ho	0.004 ± 0.001	7.0%	0.004 ± 0.001
Er	0.013 ± 0.001	7.7%	0.012 ± 0.001
Tm	0.002 ± 0.001	13.0%	0.002 ± 0.001
Yb	0.012 ± 0.001	2.5%	0.011 ± 0.001
Lu	0.002 ± 0.001	7.3%	0.002 ± 0.001

[a]Values from this study from 6 long term replicates;
[b]compilation values from Yeghicheyan et al. (2019);
and [c]certified values (µg/L).

Figure 1

Click here to download Figure: Figure 1.docx

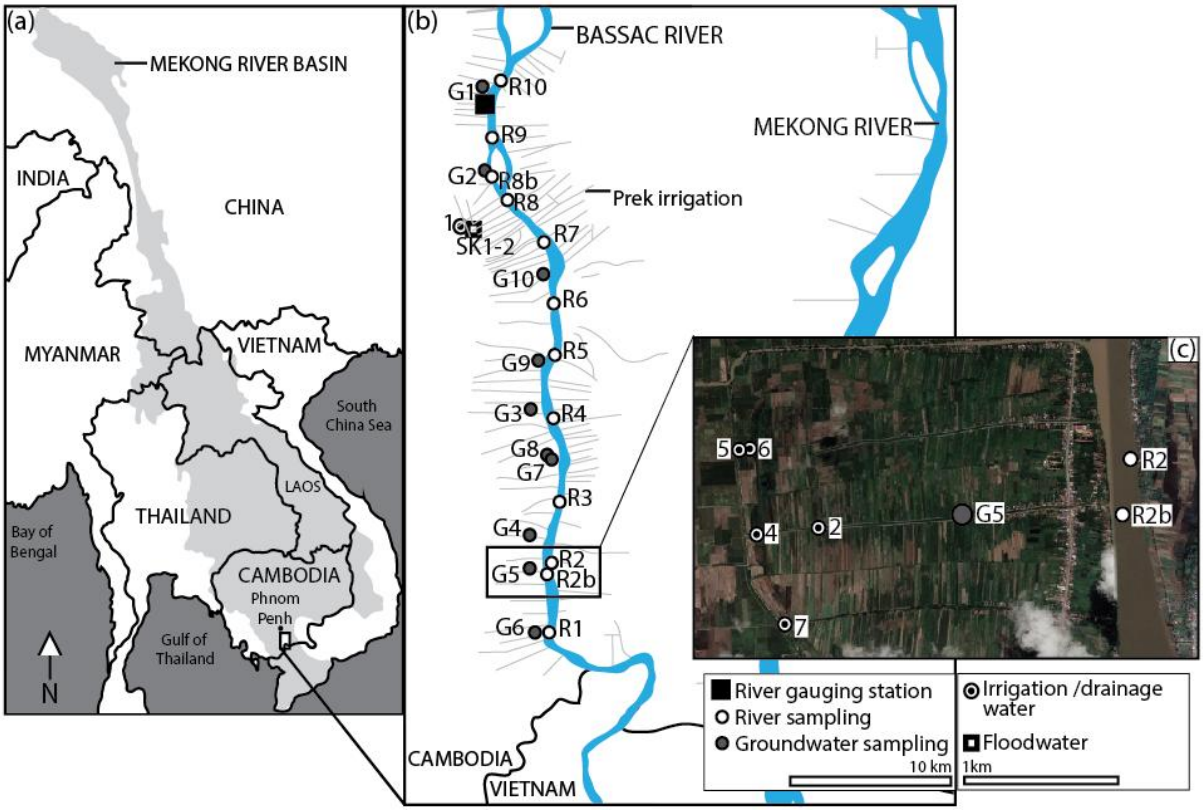

Figure 1. Map of (a) the study area located in the Cambodia Mekong Delta, Kandal province; (b) the sites for river water (R) and groundwater (G) sampling in 2018, and the river gauging station (Koh Khel) in the north of the study area; and (c) close-up view of areas sampled for irrigation/drainage prek water overlaying the image of the irrigated landscape (Google Earth, 24-June-2018).

Figure 2

Click here to download Figure: Figure 2.docx

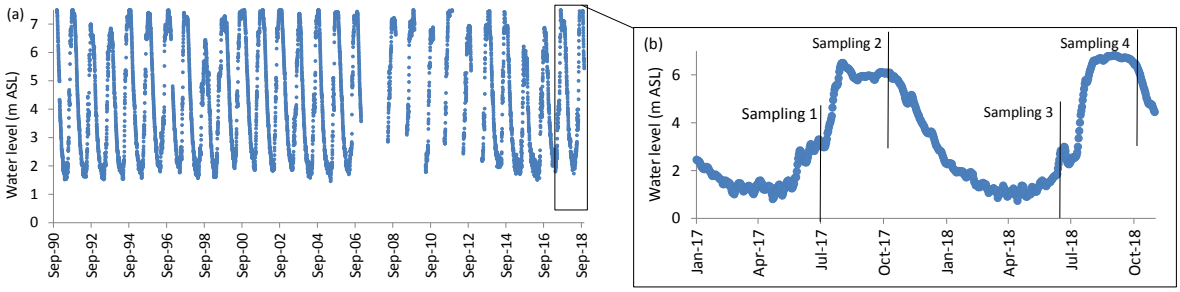

Figure 2. (a) Bassac River water levels (at Koh Khel gauging station, 33402; Mekong River Commission, 2019) from 1990 to 2018, and (b) a zoom of the river water levels during the sampling rounds in this study in 2017 and 2018.

Figure 3

Click here to download Figure: Figure 3.docx

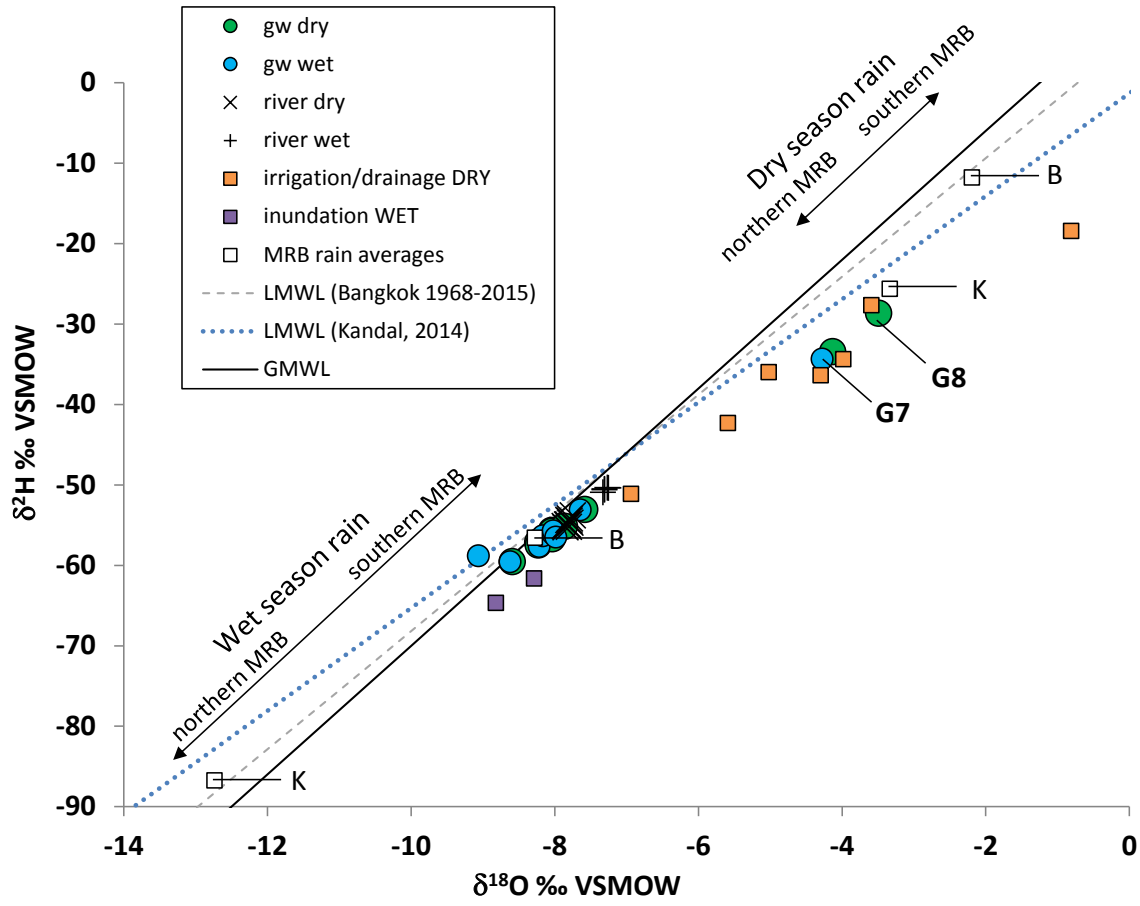

Figure 3. Stable isotope values for rain, groundwater, river, inundation, irrigation/drainage prek water collected during the dry and wet seasons 2017-2018. Values are compared with the global meteoric water line (GMWL), and the local MWLs (LMWL) from the lower delta rainfall at Bangkok (B; IAEA/WMO station 1968-2015 data) and at Kandal (K; 2014 data, Richards et al., 2018). Also presented are average values for dry season months (February and March) and wet season months (September and October) for rainfall near the southern region of the Mekong River Basin (MRB) at Bangkok, Thailand (B), and the rainfall near the northern MRB at Kunming, China (K) (data from IAEA/WMO, 2019).

Figure 4

Click here to download Figure: Figure 4.docx

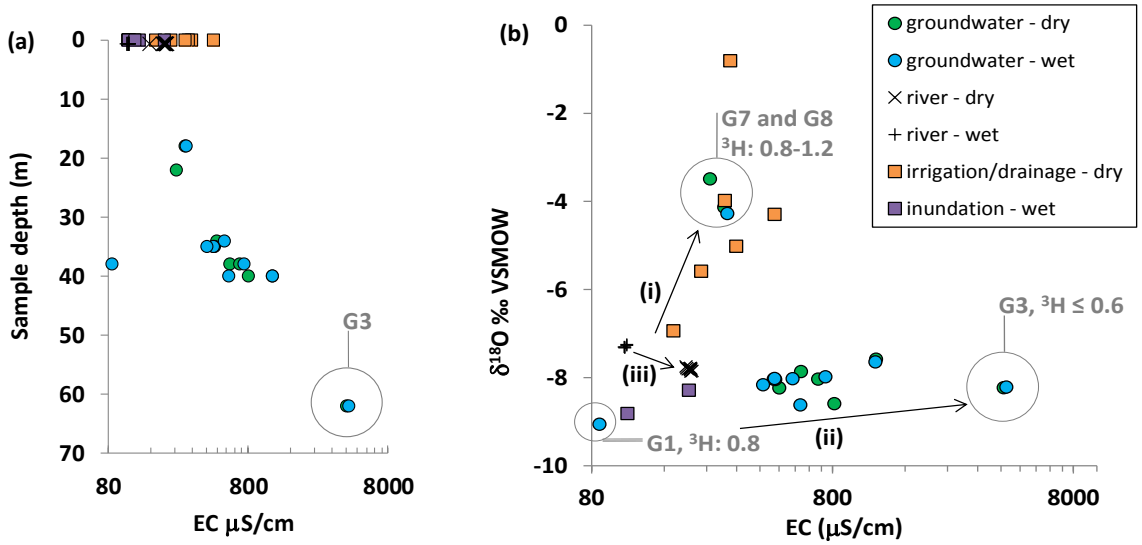

Figure 4. (a) EC values with depth to sample in the river (sampled at 0.5 m depth) and depth of the borehole in the aquifer and (b) EC and $\delta^{18}O$ values of groundwater, river, inundation, and irrigation/drainage prek water collected during the dry and wet seasons. This graph highlights 3 end-members for groundwater sampled at sites G1, G3, and G7/G8 that result from 2 main mechanisms controlling increases in groundwater EC; (i) evaporation or mixing with evaporated waters, and (ii) water-rock interactions, evapotranspiration or mixing with groundwater that had ^{3}H values below the detection limit, and 1 main mechanism increasing river EC; (iii) increased mixing with groundwater.

Figure 5

Click here to download Figure: Figure 5.docx

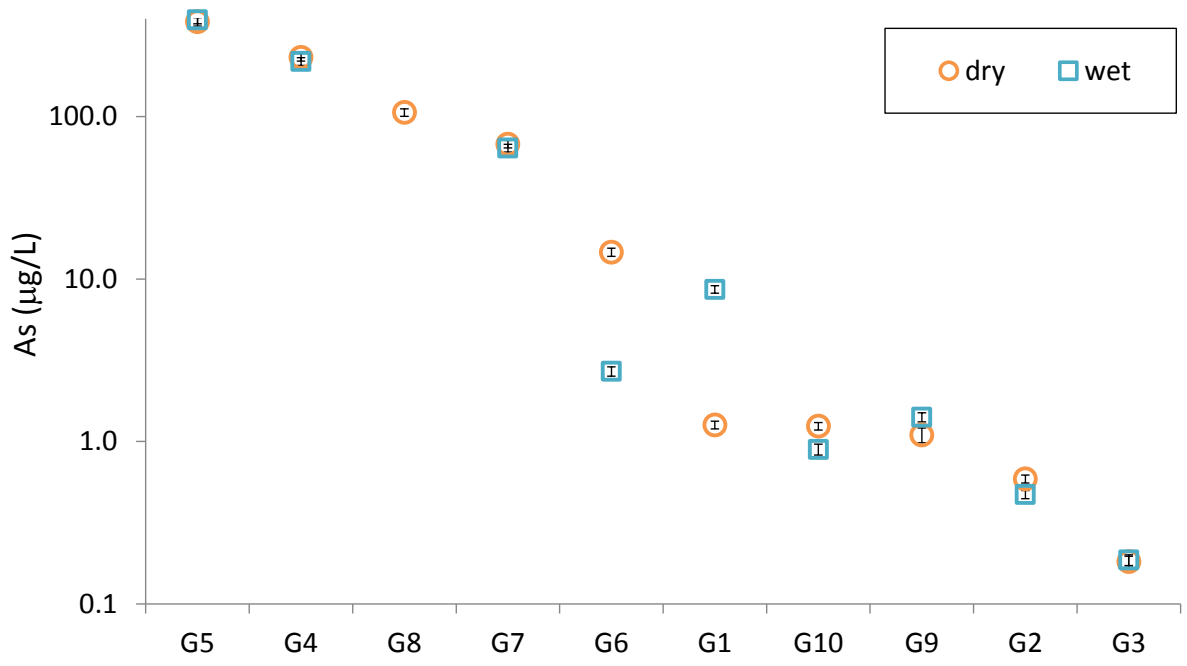

Figure 5. Dry and wet season concentrations for As (and total error bars) at each groundwater site.

Figure 6
Click here to download Figure: Figure 6.docx

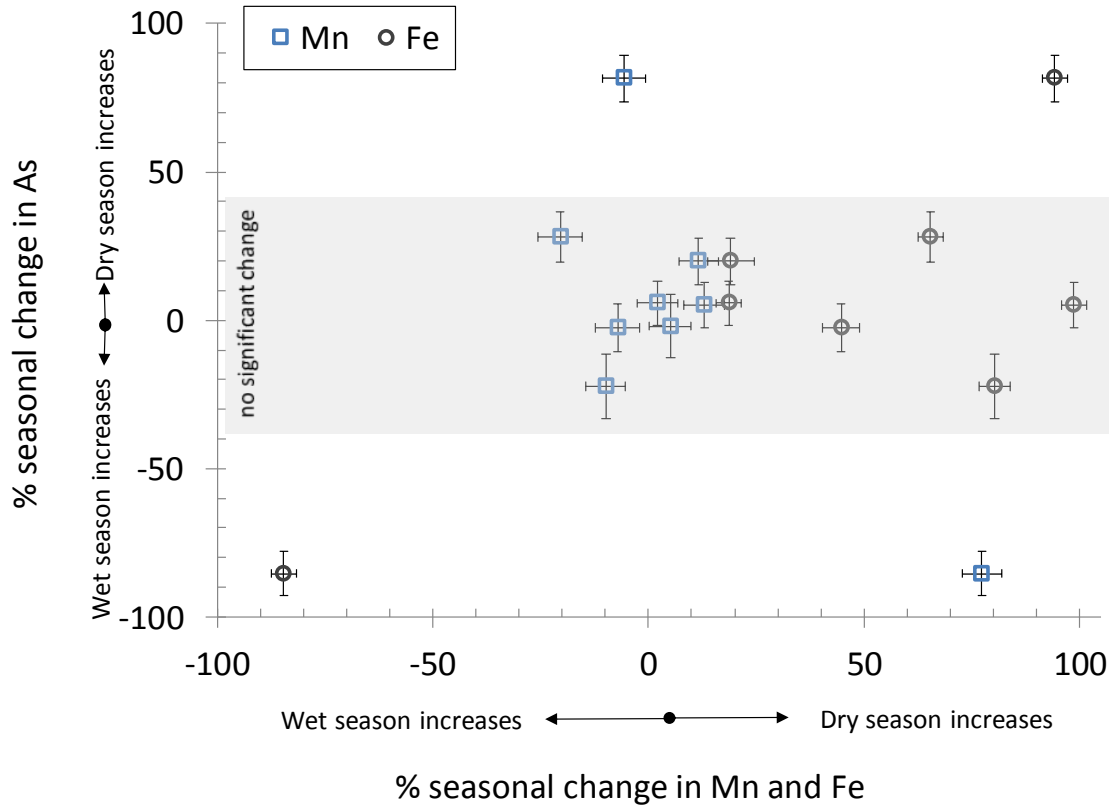

Figure 6. Percentage seasonal changes in As concentrations relative to percentage seasonal changes in Mn and Fe concentrations (with total error bars). The grey bands on both sides of the 0% change show where changes are significant for As concentrations.

Figure 7

Click here to download Figure: Figure 7.docx

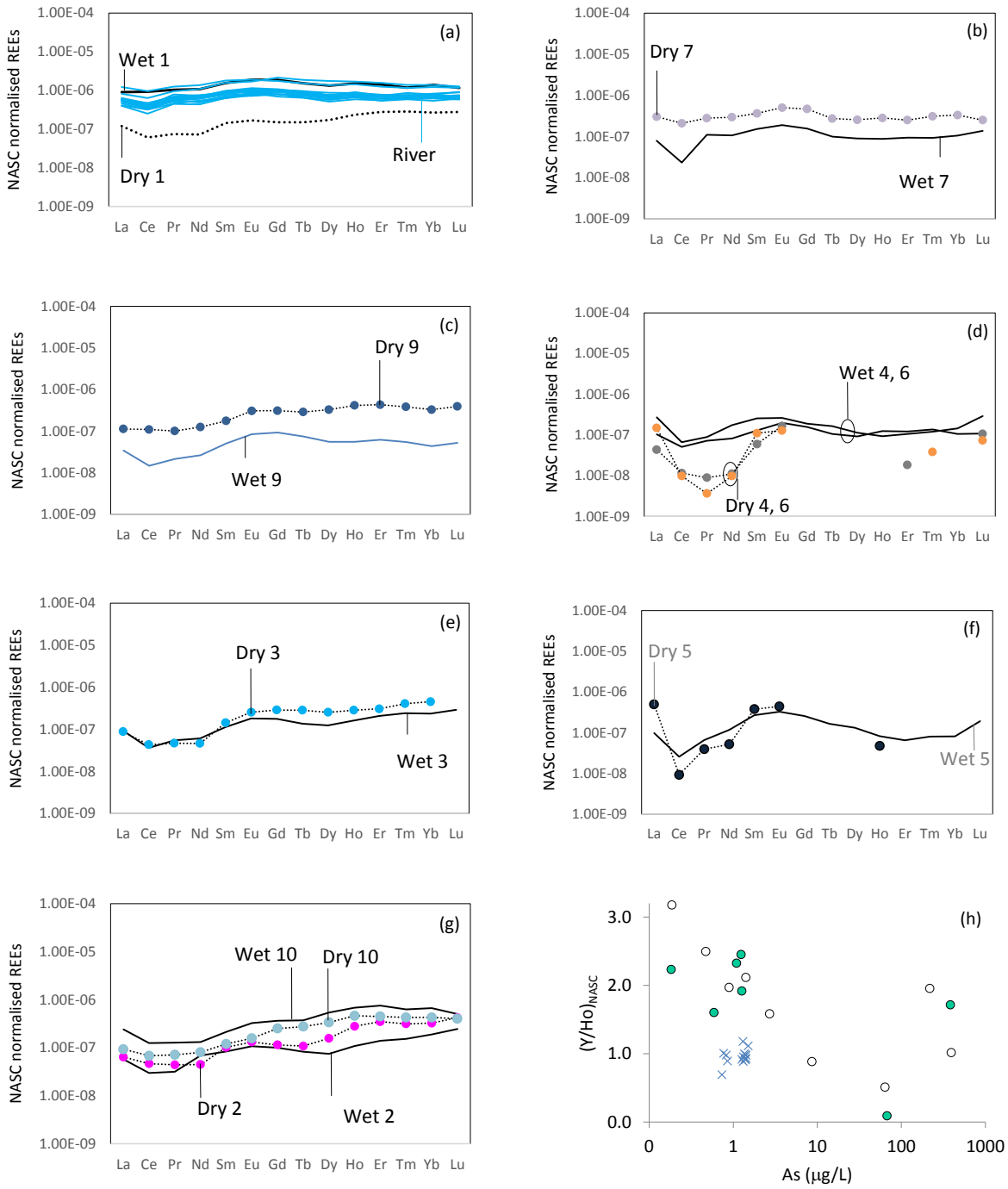

Figure 7. Rare earth element data normalised to NASC for (a) the Bassac River (dry and wet seasons) and groundwater at site G1, (b)-(g) groundwater sites G2-G10 during the dry and wet seasons, and (h) ratio of $(Y/Ho)_{NASC}$ relative to arsenic concentrations in river water (crosses), dry season groundwater (filled circles) and wet season groundwater (open circles).

Figure 8

Click here to download Figure: Figure 8.docx

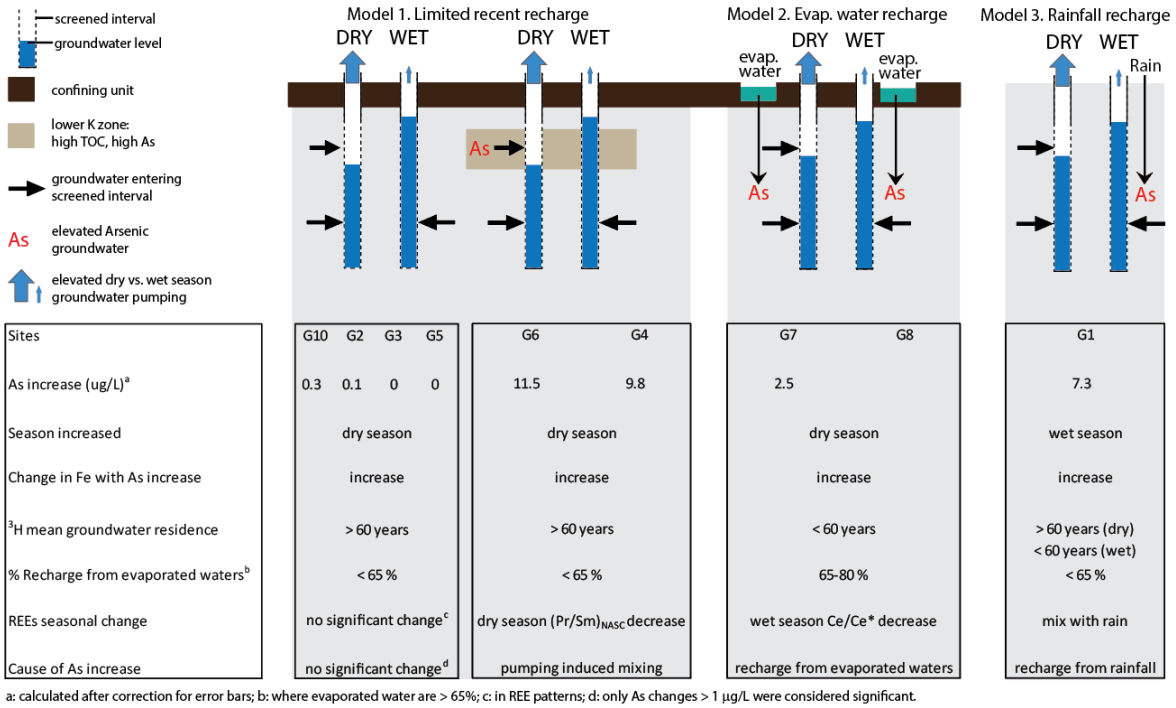

Figure 8. Simplified schematic for the models of As mobilisation proposed in this study. The seasonal changes in the groundwater elevations are unrepresentative of actual magnitudes. The dry season declines in groundwater levels were unable to be measured, and are based on anecdotal evidence and changes in seasonal groundwater elevations that were reported in a previous study by JICA (2002).